MINISTRY OF EDUCATION AND SCIENCE OF THE REPUBLIC OF KAZAKHSTAN

Nonprofit Joint Stock Company
« Almaty University of Power Engineering and Telecommunications named after Gumarbek Daukeev»

The department _____*Electric machines and electric drive*_____

«Allowed to defend »
Head of Department «Electric machines and electric drive»
___*Orzhanova Zh.K.c.t.s., associate Professor*___
(Full name, scientific degree, title)
_____ «____»_____2020y.
(sign)

MASTER'S THESIS

Theme __*Development and research of the control system of the electric drive of the mine hoist*_____

Master student _____*Dauletchin S.*_____
sign (Full name)

Thesis Supervisor _____*Almuratova N.*_____
sign (Full name.)

Reviewer _____*Sarsenbayev E.*_____
sign (Full name.)

Almaty 2020

MINISTRY OF EDUCATION AND SCIENCE OF THE REPUBLIC OF KAZAKHSTAN

Nonprofit Joint Stock Company
«Almaty University of Power Engineering and Telecommunications named after Gumarbek Daukeev»

Institute _____*Power engineering and electrical engineering*_____
Specialty _____*6M071800 – power engineering*_____
Department_____*Electric machines and electric drive*_____

Task

To complete a masters thesis
master student _____*Dauletchin S.*_____
(Full name)

Thesis theme ____*Development and research of the control system of the electric drive of the mine hoist*_____
approved by the Academic Council of the University № *122* от «*25*» *october 2018y.*

Deadline for completion of the dissertation «*10*» _____*june*_____*2020 г.*
Purpose of research: *A mine lifting system is a mechanical system consisting of engines, vessels, winding organs, gears and pulleys that are connected by ropes, shaft lines and spring couplings. They are an essential part of industry, especially in the mineral and mining fields, as well as in the housing and utilities sectors.*_____
*One of the promising directions of development of modern electric drive systems is the transition from single-engine mechanisms to mechanically or electrically interconnected multi-engine systems, this allows you to significantly reduce the weight and dimensions, increase performance, speed and reliability compared to a single-engine analog of the corresponding power.*_____
List of questions to be developed in the master's thesis or summary of the master's thesis: *In the thesis, a mathematical model of Simulink is developed and investigated of a frequency-controlled twin-engine with an electromechanical system of an asynchronous electric drive with a rigid mechanical connectiontaking into account the real discrepancy between the parameters and mechanical characteristics of the tested engines.*
_____
Recommended main literature

И.Я.Браславский, З.Ш.Ишматов, В.Н.Поляков. Энергосберегающий асинхронный электропривод. – Москва: Academa, 2004г.; Народицкий А.Г. Современное и перспективное алгоритмическое обеспечение частотно-регулируемых электроприводов. – Москва, 2014г.; Автоматизированный электропривод типовых производственных механизмов. М.И.Аксенов, А.И.Нитиевская, Г.Б.Онишенко. – М.:Наука, 2011г.

SCHEDULE
preparation of a master's thesis

Name of sections, list of issues being developed	Terms of submission to the scientific supervisor	remark
The main elements of the mine lifting system. The principle of operation of the device, classification.	01.12.2018	performed
Mathematical model of a classical unregulated two-motor asynchronous electric drive with a rigid mechanical connection	10.02.2019.	performed
Determination of the causes of the moment imbalance in an electric drive with a rigid mechanical connection	15.10.2019	performed
Influence of gaps and elasticity on the process of uneven load distribution	01.12.2019	performed
Upgrade of the lift control system	05.01.2020	performed
Modernization of the electric drive scheme of the NKMZ 2C type-5*2,3	18.03.2020	performed
Calculation of energy savings when using frequency converters	25.04.2020	performed
Reduction of power losses when using an electric drive with a frequency Converter	20.05.2020	performed

Date the task was issued _____*«08» september 2018 y.*_____

Head of department_____(*Orzhanova Zh.*____)
(sign) (full name)

Thesis Supervisor _____ _____ (_*Almuratova N.*___)
(sign) (full name.)

Task accepted for execution
Master student_____ _____(*Dauletchin S.*____)
(sign) (full name)

Annotation

In the thesis, a mathematical model of Simulink is developed and investigated of a frequency-controlled twin-engine with an electromechanical system of an asynchronous electric drive with a rigid mechanical connectiontaking into account the real discrepancy between the parameters and mechanical characteristics of the tested engines. During the tests, the causes and dependencies of the formation of the process of uneven distribution of the load were determined, including the transition to the generator mode for a frequency-controlled electric drive with vector control and speed feedback. In addition, the fact of the influence of gap formation and elasticities of gears on the process of formation of an imbalance of moments was established..

Modeling of the electromechanical system showed that a twin-motor asynchronous gear drive generates a significant imbalance in the distribution of the total load between the drives and reaches 13-20%, what indicates the need for an extension with the SVN scheme; tests OF the svn "lead-lead" on the lift mechanism confirmed high technical indicators of load distribution, both in static and in transient operation. The accuracy of load distribution, as in experiments, is ~1-2%. Thanks to the structural changes made and the use of the developed SVN "leading-leading", vibration and vibrations of the mechanism are significantly reduced, which means that the durability has increased.

On the example of a mine lifting machine of the NKMZ 2C-5*2,3 type, the electric drive system is studied, and the problem of energy saving is considered: the calculation of energy savings and reduction of losses in the electric drive when replacing the rotary station of an electric motor with a phase rotor with an adjustable electric drive is carried out, which is the purpose of the work. The economic effect of using frequency converters is shown: reduction of equipment breakdowns and accidents, more precise regulation of acceleration and deceleration of the skip; energy savings of 9.8%; and all the sliding power of the rotor of electric motors through the frequency Converter is returned to the supply network of 6 kV 50 Hz, and is not spent on heating the rotor resistances and heating the motor.

Андатпа

Диссертациялық жұмыста механикалық байланысы бар асинхронды электр жетектің электр механикалық жүйесі бар жиіліктік-реттелетін екі қозғалтқышты Simulink математикалық моделі әзірленді және зерттелді, сыналатын қозғалтқыштардың параметрлері мен механикалық сипаттамаларының нақты айырмашылығы ескеріледі. Зерттеу барысында жүктемені бір келкі емес бөлу процесінің қалыптасуының себептері мен тәуелділігі анықталды, оның ішінде векторлық басқарумен және жылдамдық бойынша кері байланысы бар жиіліктік-реттелетін,электржетек үшін генераторлық режимге ауысу. Сондай-ақ, тісті берілістердің саңылау түзілуінің және серпімділігінің сәттердің теңгерімсіздігін қалыптастыру процесіне әсер етуі анықталды.

Электр механикалық жүйені модельдеу тісті берілісі бар екі қозғалтқышты асинхронды жетек жетектер арасында қосынды жүктемені таратуда айтарлықтай дисбалансты қалыптастырып, 13-20%-ға жетеді, бұл СВН СУ схемасымен толықтыру қажеттілігін көрсетеді; көтергіш механизміндегі "жетекші-жетекші" СВН сынақтары статикалық және ауыспалы жұмыс режимінде жүктемені бөлудің жоғары техникалық көрсеткіштерін растады. Жүктемені үлестіру дәлдігі, эксперименттер сияқты ~1-2% құрайды. Енгізілген конструктивті өзгерістер мен әзірленген "жетекші-жетекші" СВН-ны пайдалану арқасында механизмнің дірілі мен тербелісі айтарлықтай азаяды, демек, ұзақ мерзімділік артты.

НКМЗ 2Ц-5*2,3 типті шахталық көтергіш машина мысалында электр жетегі жүйесі зерттелді, энергия үнемдеу мәселесі қарастырылды: электрқозғалтқыштың роторлық станциясын фазалық ротормен реттелетін электржетекке ауыстыру кезінде электрқозғалтқыштың шығынын азайту және электрқозғалтқыштың үнемдеу есебі жүргізілді, бұл жұмыстың мақсаты болып табылады.. Жиілік түрлендіргіштерді қолданудың экономикалық әсері көрсетілген: жабдықтың сынуы мен апаттарын қысқарту, скиптің үдеуін және тежелуін дәл реттеу.; электр энергиясын 9,8%-ға үнемдеу; сондай-ақ, жиілік түрлендіргіші арқылы электр қозғалтқыштары роторының сырғуының барлық қуаты роторлық кедергілердің қызуына және электр қозғалтқышының қызуына емес, 6 кВ 50 Гц қоректендіргіш желісіне қайтарылады.

Аннотация

В диссертационной работе разработана и исследована математическая модель Simulink частотно-регулируемого двухдвигательного с электромеханической системой асинхронного электропривода с жесткой механической связью, учитывающая реальное расхождение параметров и механических характеристик испытуемых двигателей. В ходе испытаний определены причины и зависимости формирования процесса неравномерного распределения нагрузки, в том числе и перехода в генераторный режим для частотно-регулируемого электропривода с векторным управлением и обратной связью по скорости. Кроме этого был установлен факт влияния зазорообразования и упругостей зубчатых передач на процесс формирования дисбаланса моментов.

Моделирование электромеханической системы показало, что двухдвигательный асинхронный привод с зубчатой передачей формирует значительный дисбаланс в распределении суммарной нагрузки между приводами и достигает 13-20%, что говорит о необходимости в дополнении СУ схемой СВН; испытания СВН «ведущий-ведущий» на механизме подъемника подтвердили высокие технические показатели распределения нагрузки, как в статическом, так и в переходном режиме работы. Точность распределения нагрузки, как и в экспериментах составляет ~1-2%. Благодаря внесенным конструктивным изменениям и использованию разработанной СВН «ведущий-ведущий» значительно уменьшается вибрация и колебания механизма, значит, повысилась долговечность.

На примере шахтной подъемной машины типа НКМЗ 2Ц-5*2,3 исследована система электропривода, рассмотрена проблема энергосбережения: проведен расчет экономии электроэнергии и уменьшения потерь в электроприводе при замене роторной станции электродвигателя с фазным ротором на регулируемый электропривод, что является целью работы. Показан экономический эффект применения частотных преобразователей: сокращение поломок и аварий оборудования, более точное регулирование разгона и торможения скипа; экономия электроэнергии составляет 9,8%; а также вся мощность скольжения ротора электродвигателей через преобразователь частоты возвращается в питающую сеть 6 кВ 50 Гц, а не затрачивается на нагрев роторных сопротивлений и нагрев электродвигателя.

Designations and abbreviations

AM	- asynchronous motor
MLP	- mine lifting plant;
MD	- master drive;
SD	- slave drive;
E	- electromotor;
IS	- intensity setter;
VC	- voltage converter;
CC	- current converter;
R	- reducer;
SC	- speed controller;
CC	- current controller;
SM	- synchronous motor;
EDCS	- electric drive control system;
ACS	- automatic control system;
LBS	- load balancing system;
ACS	- automatic control system;
EDCS	- electric drive control system;
FC	- frequency converter;
SRCS	- starting resistor-contactor stations
DBS	- dynamic braking stations
DFC	- direct frequency converter
SC	- speed controller

Content

Introduction

Relevance of the topic. A mine lifting system is a mechanical system consisting of engines, vessels, winding organs, gears and pulleys that are connected by ropes, shaft lines and spring couplings. They are an essential part of industry, especially in the mineral and mining fields, as well as in the housing and utilities sectors.

One of the promising directions of development of modern electric drive systems is the transition from single-engine mechanisms to mechanically or electrically interconnected multi-engine systems, this allows you to significantly reduce the weight and dimensions, increase performance, speed and reliability compared to a single-engine analog of the corresponding power.

A significant disadvantage of this solution is that the mechanical characteristics of electric motors of the same type are not identical. In the case of mechanically interconnected systems, this leads to an uneven distribution of loads between the drives in static and dynamic operating modes, and therefore to an overload of the motor, which has a more rigid mechanical characteristic, as well as to complicate the dynamics and additional loads of an oscillatory nature, which increase the wear of gears, cause vibration and make it difficult to achieve the required accuracy of the mechanism. This is especially important for frequency-controlled drives, which usually have control systems with feedback, which increases the negative effect of misalignment.

These negative factors are caused by zazhoroobrazovanie, the presence of multi-stage gears, polispastov, gear couplings, etc., and are sources of elastic vibrations in the mechanical part. An important reason that strengthens and affects almost all negative processes occurring in the mechanical part of lifts is the inconsistency of the operation of the lift mechanism drives. Due to the increased vibration activity and accelerated wear of one of the most expensive parts of lifting mechanisms, namely gearboxes, defects lead to the need to reduce operating speeds (up to 39%), and therefore to a decrease in the performance of the mechanism.

Also, in such installations, the main consumer of electricity is an electric drive (up to 70% of the generated electricity). Significant savings in electrical energy can be achieved using adjustable electric drives, they will also solve a number of technological problems. In this regard, this dissertation will consider the electric drive system of a mine lift.

The current state of development of computer technology and control tools, the development of an automated electric drive based on asynchronous motors allow us to solve current problems - the creation of energy-saving systems for controlling lifting installations.

The purpose of this work is to develop a control system for the electric drive of a mine lifting plant and calculate energy efficiency when using frequency converters.

In this regard, the following ta**sk**s are set:

1) Construction of an adequate mathematical model of a two-motor asynchronous electric drive with mechanical coupling;

2) Investigation of the causes and regularities of uneven load distribution in a frequency-controlled drive with vector control using experiments on a mathematical model and experimental bench studies:

3) Development of a system for equalizing static and dynamic loads in the presence of elastic connections and gaps, as well as a method for parametric tuning of a multi-motor frequency-controlled asynchronous electric drive, debugging on a stand and testing as part of a SU with lift drives;

4) Calculate the energy efficiency of using a frequency converter.

Object of research – electric drive systems for mine lifts based on asynchronous motors.

The subject of the research schemes and control laws of electric drives of shaft hoist installation.

Scientific novelty of the research: a mathematical Simulink model has been developed for the study of transients, in the course of tests, the causes and dependencies of the formation of the process of uneven load distribution, including the transition to generator mode for a frequency-controlled electric drive with vector control and speed feedback were determined.

Practical value: the developed control system of the electric drive allows to improve the characteristics for optimal operation of the mechanism, as well as the use of frequency converters give quite significant indicators of energy saving.

Testing the work: The materials of the dissertation were discussed and reported at the conference of undergraduates and doctoral students of AUPET and in the collection of materials international scientific and practical conference "Scientific potential of modern youth" may 14-15, 2020, Nur-Sultan, 2020.

1 The main elements of mine hoisting installations

1.1 Device, principle of operation and classification of mine hoisting installations

In the practice of developing mineral deposits by underground mining, the single-rope mine hoisting installations become most common. Single -rope vertical shaft lifting installation (SLI) (picture 1.1) consists of a shaft lifting machine 5, lifting ropes 2, envelope guide pulleys 4. Lifting vessels suspended from lifting ropes 1, in which the lifting of minerals, descent or lifting of people, materials and equipment. In deep mine hoisting installations, a tail (balancing) rope can be suspended from the vessels 3[4].

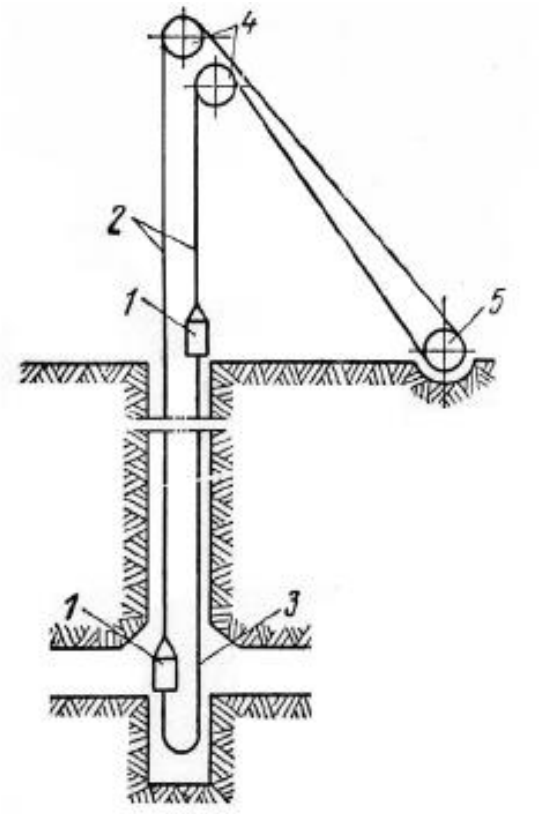

Picture 1.1 - Diagram of a vertical multi-rope shaft lift installation

To the mine lifting machine through the reducer or directly transmitted torque from the shaft of the lifting motor lifting ropes are tied to the winding body of the mine lifting machine in such a way that when they rotate, one rope is wound, and the other is twisted, and when one vessel is lifted, the second is lowered. As a result, the own weight of the lifting vessels is balanced. On mine lifting installations with a counterweight, one lifting vessel is replaced by a counterweight, the weight of which is equal to the weight of the vessel plus half the weight of the calculated load lifted in it. Mine lifting units are classified according to the type of drive (with or without gearbox):

а) alternating current:

– induction motor with phase rotor (with metal or liquid rheostat in rotor circuit);

– induction motor with squirrel cage rotor and frequency converter:

б) direct current,:

– driven by generator-engine system;

– with the drive system of the thyristor converter engine.

By type of lifting vessels — cage, skip and bucket.

To ensure the directional movement of lifting vessels mine shafts are equipped with reinforcement. Reinforcement is a rigid spatial structure placed along the entire length of the barrel the directional movement of vessels is provided by conductors. There are rigid and flexible conductors. Conductors flexible reinforcement are stretched in the trunk of the ropes.

As rigid conductors, rail rolling, various metal profiles (most often welded from two corners – conductors of box section) and wooden bars are used.

Mine lifting machines are installed on a reinforced concrete Foundation and fastened with anchor bolts. The machines are made in the form of a welded structure with screw cutting of the shell under the rope. Large lifting machines with a drum diameter of 4 m or more are equipped with one split, two cylindrical or split bicylindro-conical winding body. One drum of two-drum machines and the main (most) part of the split winding organs are rigidly connected to the shaft. This drum (part of the winding organs) is called jammed. The second (adjustable) drum or adjustable part of the split drum is mounted on the shaft on bearings and has the ability to rotate. The drums are connected to the shaft by a special permutation mechanism.

The permutation mechanism allows you to detach the adjustable drum or the adjustable part of the drum from the shaft of the mine lifting machine and perform operations to replace the rope, adjust the length of the rope by rotating one drum or the jammed part of the drum.

Mine lifting machines are equipped with brake devices pad type.. The drive of brake devices of small mine lifting machines (diameter of drums 1,2 m, 1,6 m and 2,0 m) - spring-hydraulic. Single and double drum mine lifting machines with a drum diameter of 2, 5 m, 3.0 m and 3.5 m, as well as multichannel machines are equipped with spring-pneumatic brakes.

The brake system of large mine lifting machines NMBP consists of pneumatic brake drive, Executive body and brake control panel. To improve reliability, each machine has two actuators, each with its own drive.

The brakes operate independently of each other.

Pneumatic brake actuator (picture 1.2) consists of two brake beams 1 with press mass pads 2, two vertical racks 3, mounted on supports 4, three triangular arms 5, thrust, 6 and 7. Thurts 6 it consists of two parts, connected by adjusting nut 8. The brake has a control rack 9 and stops 10 and 11.

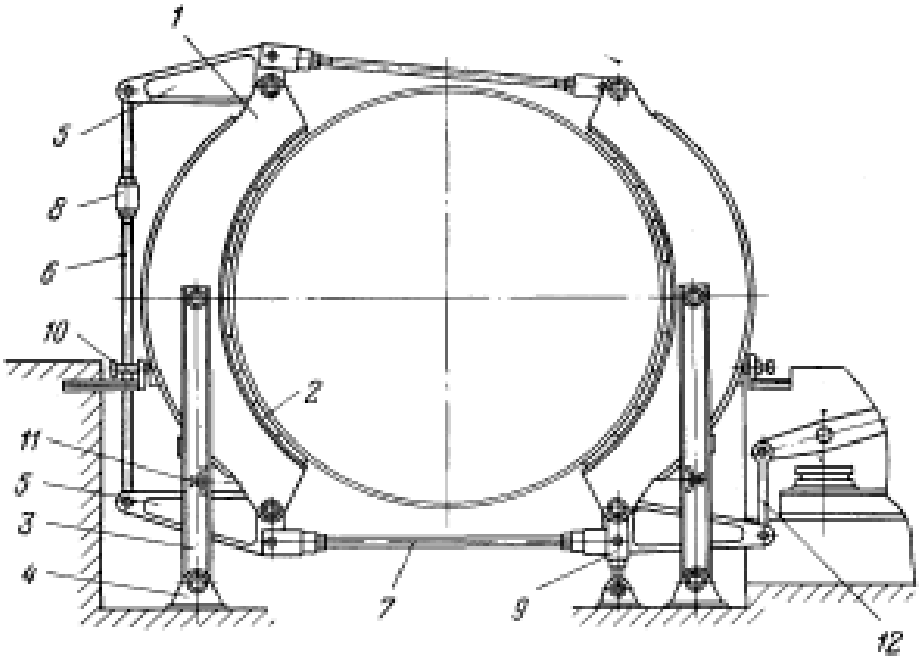

Picture 1.2 - The Executive body of the brakes mine winders

The force of the brake drive is transmitted through the vertical thrust 12, system of levers 5 and rods 6 and 7 on brake beams 1, which press the brake pads against the rim, producing braking of the lifting machine. Disinhibition of the machine is due to the unbalance of the weight of the lever system elements and the weight of the brake drive elements: piston, rod, differential lever.

The brake actuator comprises a service braking cylinder, a safety braking cylinder, the piston of which is connected to the rod with the brake load. The force from the cylinder pistons is transmitted to the vertical thrust of the brake actuator through the differential lever.

1.2 Drive of mine lifting units

The electric drive of mine lifting installations is carried out by electric motors of direct or alternating current. Most mine lifting units are equipped with induction motors with a phase rotor with a metal or liquid rheostat, which is due to their low cost, ease of maintenance and high operational reliability.. Due to the high speed of asynchronous motors, their connection is carried out through a reducer. The scheme of the asynchronous drive with a phase rotor is shown in the figure 1.3. Contactors of reversers B and H carry out a change in the direction of rotation of the engine M [6].

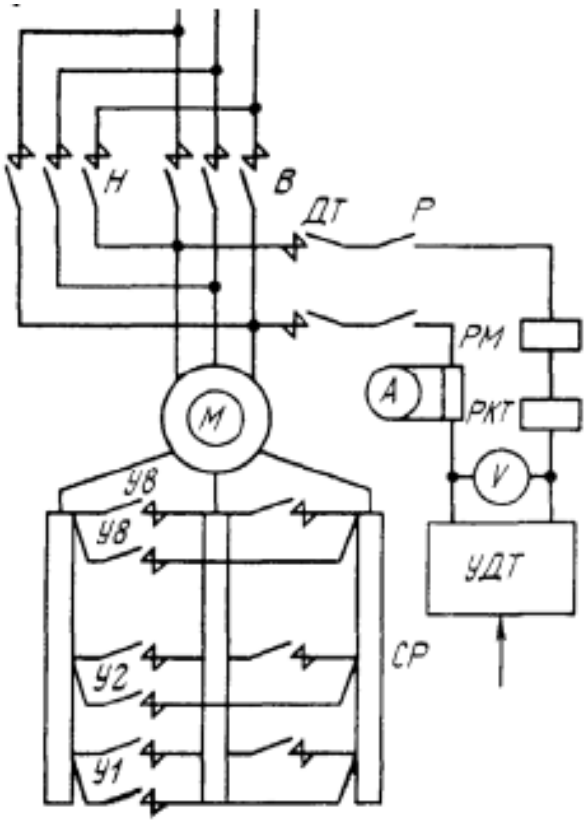

Picture 1.3 - Scheme of an asynchronous drive

Adjustable resistance is used to control the frequency rotating speed of motor AR, included in the rotor circuit and changed when the rotor contacts U1–U8.

Asynchronous drives of mine lifting machines are equipped with dynamic braking, adjustable DC power supply UDT , the motor is connected to the motor stator via a dynamic braking contactor BC when contacts are disconnected B and H.

The dependence of the engine speed on the torque developed by it is called mechanical characteristics. The mechanical characteristics of the asynchronous drive are shown in the picture 1.4.

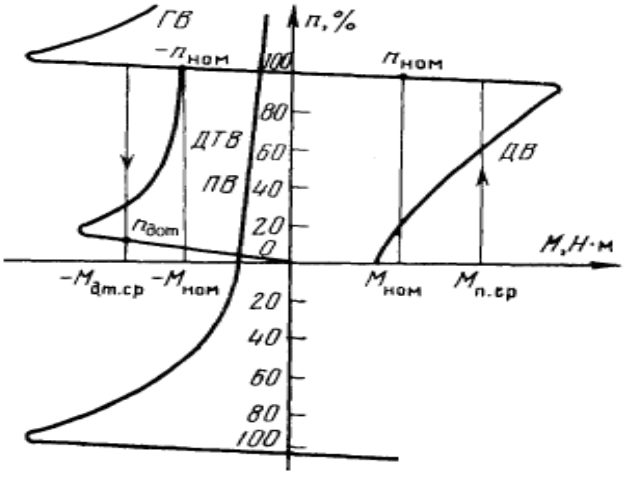

Picture 1.4 - Mechanical characteristics of an induction motor

When rotating the winding body in the "forward" direction, the asynchronous motor can operate in the following modes:

– motor mode (field DB, picture 1.4) – the direction of movement of vessels coincides with the direction of the moment developed by the engine. The torque is created by the interaction of the rotor current with the rotating magnetic field;

– generator braking mode GB – the motor rotates by moment, created by the tension difference of the lifting ropes. The braking torque, which prevents the acceleration of the system, is created by the interaction of the rotor current with the rotating magnetic field. In this mode the active power is transferred to the network;

– braking by counter-connection CC – extremely rare mode when braking is carried out by turning on the engine in the opposite direction, that is, the magnetic field of the stator of the engine and the rotor rotate counterclockwise;

– dynamic braking mode DBB – created by connecting the stator windings to a DC source. The braking moment is created by the interaction of the rotor current with a fixed magnetic field.

Asynchronous motors have relatively rigid natural mechanical characteristics with nominal slip $S_{nom} = 0,02…0,03$.

To perform the diagrams of the movement of the mine lifting machine, the motor accelerates c $n_{motor} = 0$ up to rated speed by average starting torque $M_{п.average}$ (picture 1.4). At this speed with positive static torque M_s, equal to the nominal M_{nom}, movement to the point is carried out + $П_{nom}$. Generator braking is used when lowering the load. At rated static torque M_{nom} the motor operates on a natural characteristic at the point - $П_{nom}$. Deceleration of the machine from maximum speed to low speed can be carried out in dynamic braking mode using a mechanical characteristic with an average braking torque MDT CP from the point - $П_{nom}$ up to point $n_{дот}$.

The mechanical characteristics of the induction motor when connecting the rotor resistors are shown in picture 1.5.

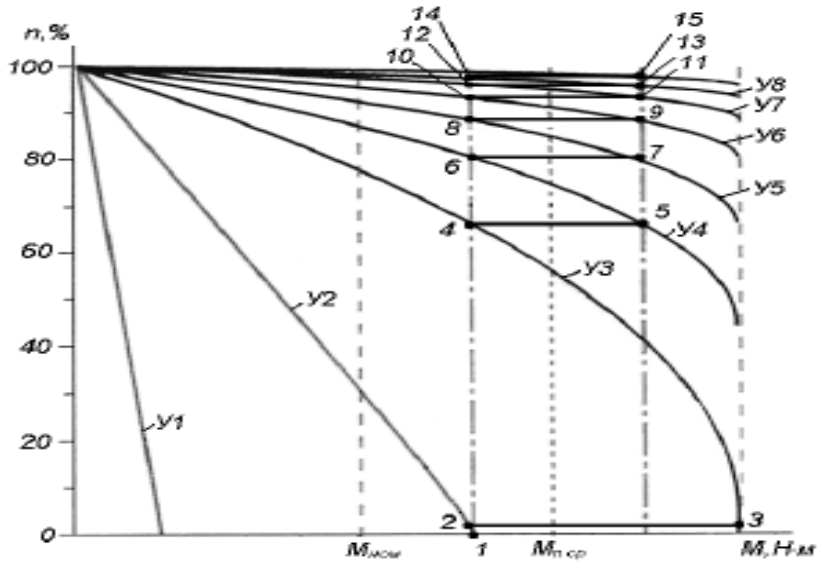

Picture1.5 - Mechanical characteristics of asynchronous motor with phase rotor

At the maximum value of the rotor resistances the torque of the motor is determined by the characteristic U1(У1). It provides a smooth application of the load to the shaft of the lifting machine. On the second stage (characteristic U2(У2)) there is a starting of the car and acceleration along the line 1 – 2. When the third stage is turned on, the engine torque increases abruptly along the line 2-3 and the lifting unit accelerates along the line 3-4.

Further removal of the rotor resistances provides a stepwise increase in speed along the broken line 4, 5, 6, 7, ...,14, 15 up to rated speed n_{nom}.

In the practice of operation of mine lifting installations the maximum speed of vessels is limited. In this case, not all contactors of the control station are switched on, and the lifting motor operates on one of the artificial characteristics. For example, when the engine is running on the characteristic U4(У4) the motor at rated torque on the shaft will rotate at a frequency of n U4(У4). Accordingly the movement of lifting vessels will occur at a lower speed. In this case, the lifting motor has a "soft" characteristic and the speed will change when the moment of resistance on the shaft of the lifting machine changes.

Powerful mine lifting units are equipped with a DC drive. Currently in operation are installations driven by the generator-motor system (the power circuit is shown in picture 1.6) and driven by the thyristor Converter–motor system.

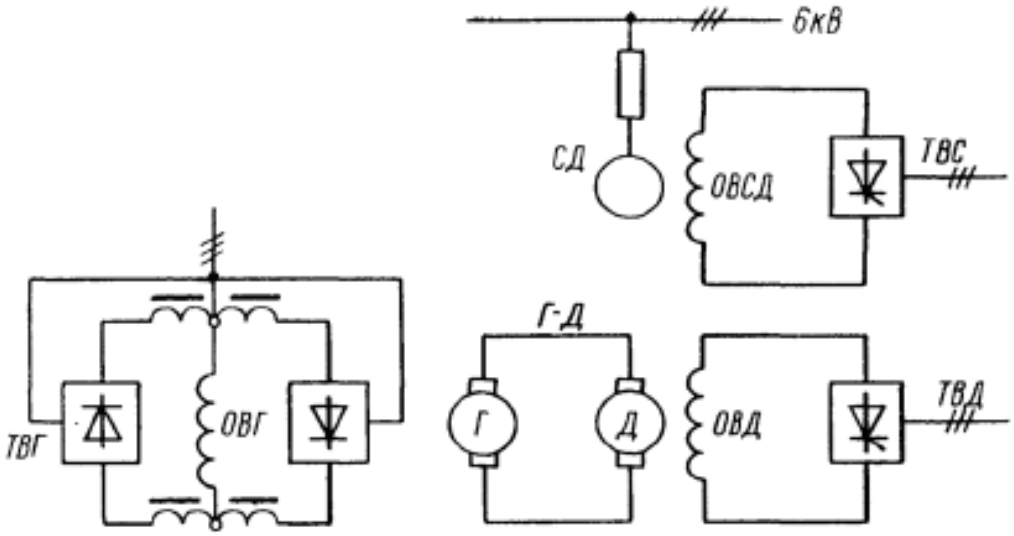

Picture 1.6 - The power scheme of the drive system (E–G)

The mechanical characteristics of the DC motor are determined by the dependence

$$n_{дв} = \frac{U}{c_e \Phi} - \frac{MR_я}{c_e c_м \Phi^2}, \quad (1.1)$$

Where U – the voltage on the armature of the motor; $R_я$ - motor anchor chain resistance; M – moment on motor shaft; Φ – the magnetic flux of the motor; c_e, $c_м$ - design characteristics of the engine

Graphs of the dependence of the engine speed on the torque on its shaft are shown in picture 1.9. The slope of the characteristics is determined by the voltage drop in the motor anchor circuit.

In the drive of mine lifting machines by the system E–G engine speed control o f frequency E carried out with a constant magnetic flux of the engine Φ = const by changing the generator voltage supplied to its armature G by regulating its excitation current.

The generator excitation winding is powered by a reversible thyristor Converter. The reversible drive Of the E–G mine hoisting machines is controlled in four quadrants of mechanical characteristics. The change in the linear speed of lifting and driving forces on the winding body of the mine lifting machine corresponds to the change in the speed and torque on the motor shaft on the mechanical characteristics of the drive (picture 1.7).

Acceleration of the system when lifting the load to the nominal speed is carried out along the lines of 0–1–2–3. Point 1 defines the moment M_e, generated by the lifting engine. Under the action of the difference between the moments of the motor and the moment of resistance M_s there is also an acceleration of the system on line 1-2.

At the point 3 $M_d = M_s$ and further movement occurs at a constant speed. Deceleration of the system at the end of the lift can occur in the motor (lines 3-4-7-8) or generator (lines 3-4-5-6-7-8) mode of operation of the engine

At point 8 the vessels are drawn at a constant speed. При этом $M_d = M_s$.

When the load is lowered, the lifting motor operates in the generator mode (the second quadrant of the mechanical characteristic). Change of moment M_d when you perform a given law of motion is similar.

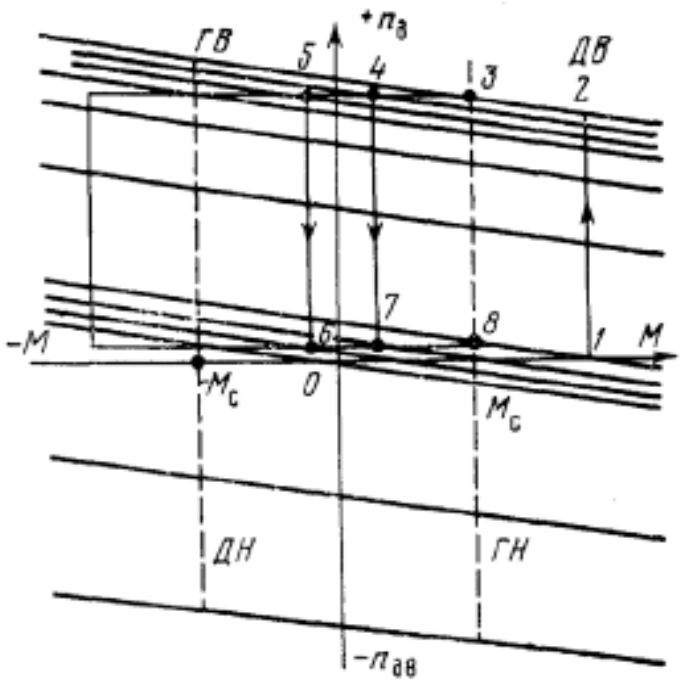

Picture 1.7 - Mechanical characteristics of the engine

Drive by system TC-E (thyristor converter engine) currently it is implemented in two fundamentally different schemes:

а) with reverse on the anchor chain of the engine (the power circuit is shown in the picture1.8, a);

б) with reverse on the motor excitation circuit (picture 1.8, b).

System TC-E with reverse on the anchor chain of the engine, as well as the drive system E–G, provides control of the movement of lifting vessels by changing the magnitude and polarity of the input voltage of the converter.

Mechanical characteristics of the drive system TC-E (picture 1.9) similar to drive dependencies E–G. The exception is the intermittent current zone, bounded by a dashed line in which the characteristics are distorted.

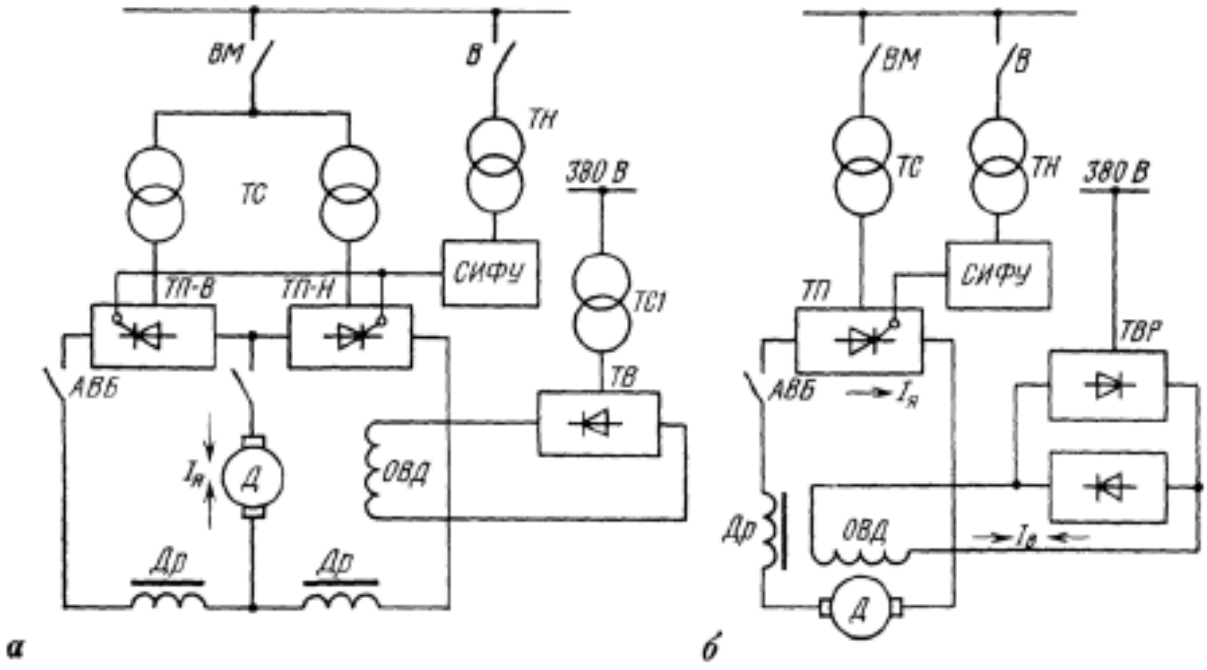

Picture 1.8 - The power circuit of the drive system TC-E

When the lifting motor is operating in generator mode, the thyristor Converter of the anchor circuit switches to inverter mode, providing DC-to-AC conversion and energy transfer from the motor circuit to the supply network.

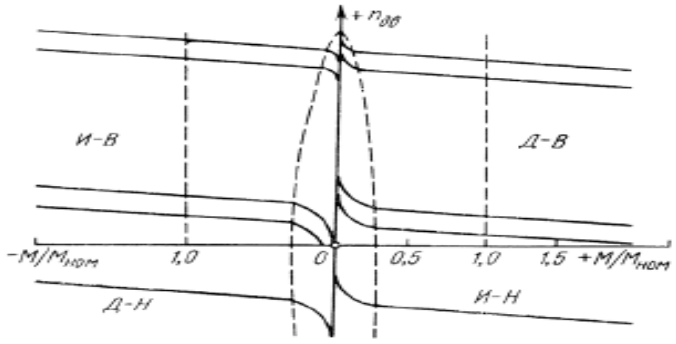

Picture 1.9 - Mechanical characteristics of the drive system TC-E

In an automated skip shaft lifting unit with an asynchronous motor the operation cycle consists of the following modes: when lifting loads, the machine operates in motor mode, then before entering the unloading curves, dynamic braking is performed to a predetermined reduced speed; before stopping, when the skip is in the unloading curves, the reach is made in the motor mode at a reduced speed. In this case, the statistical load of the engine on the cycles varies slightly. Reaching the skip is carried out during the period when it enters the unloading curves, before the final stop and unloading. In addition to the main operating mode, the electric drive must provide a rise with a reduced speed, which is used for testing the installation, adjusting the equipment and checking the ropes.

Conclusion: The first chapter describes the main elements of mine lifting machines, their classification, operating principle, as well as the mechanical characteristics of the asynchronous motor with a phase rotor and DC motor and drive. Shows a diagram of the installation with the motors in the system generator–motor and drive system thyristor converter–motor.

2 Mathematical model of a classic unregulated twin-motor asynchronous electric drive with rigid mechanical connection

The mathematical model of a frequency-controlled asynchronous drive must satisfy the following requirements [15]:

1. Simplicity in implementation.
2. Accounting for the effect of iron saturation of the magnetic core on the parameters of an asynchronous motor.
3. Accounting for frequency and voltage regulation laws frequency converter.
4. Taking into account the mechanical characteristics of the load moment and the brake device.

For mathematical model frequency-controlled asynchronous motors a mathematical model of a generalized machine in a synchronous coordinate system is used *u*,*v* [15]. The coordinate system u, v allows you to most simply change the phase voltage amplitude and frequency of the if in time, regardless of each other, according to any given law:

$$\left.\begin{aligned} u_{su} &= i_{su}\cdot r_s + \frac{d\psi_{su}}{dt} - \omega_x\cdot\psi_{sv};\\ u_{sv} &= i_{sv}\cdot r_s + \frac{d\psi_{sv}}{dt} + \omega_x\cdot\psi_{su};\\ 0 &= i_{ru}\cdot r_r + \frac{d\psi_{ru}}{dt} - (\omega_x-\omega_r)\cdot\psi_{rv};\\ 0 &= i_{rv}\cdot r_r + \frac{d\psi_{rv}}{dt} + (\omega_x-\omega_r)\cdot\psi_{su};\\ M_{эм} &= M_c(t) + \frac{J_\Sigma}{p}\cdot\frac{d\omega_r}{dt}, \end{aligned}\right\} \quad (2.1)$$

Where: u_{su}, u_{sv} – voltages; i_{su}, i_{sv}, i_{ru}, i_{rv} – currents, r_s, r_r – resistances; ψsu, ψsv, ψ_{ru}, ψ_{rv} – flow coupling of the stator and rotor windings of a generalized machine;

Mэм and *Mc*(*t*) – electromagnetic and load moments;

*J*Σ – total moment of inertia,

p – the number of pairs of motor poles;

ωx and ωr – the angular rotation frequency of the coordinate system u, v and the rotor.

The coordinate system u, v rotates synchronously with the magnetic field of the stator winding with angular frequency

$$\omega_x = 2\pi f_x, \tag{2.2}$$

Where fx – the output frequency frequency converter.

The system of differential equations (1) is supplemented in matrix form by the equations of flow coupling of the stator and rotor windings:

$$\begin{vmatrix} \psi_{su} \\ \psi_{ru} \end{vmatrix} = \begin{vmatrix} L_s & L_m \\ L_m & L_r \end{vmatrix} \times \begin{vmatrix} i_{su} \\ i_{ru} \end{vmatrix}; \tag{2.3}$$

$$\begin{vmatrix} \psi_{sv} \\ \psi_{rv} \end{vmatrix} = \begin{vmatrix} L_s & L_m \\ L_m & L_r \end{vmatrix} \times \begin{vmatrix} i_{sv} \\ i_{rv} \end{vmatrix}. \tag{2.4}$$

Full inductive reactance of the phase windings of the stator L_s and rotor L_r:

$$\left.\begin{aligned} L_s &= L_{\sigma 1n} + L_m, \\ L_r &= L_{\sigma 2n} + L_m, \end{aligned}\right\} \tag{2.5}$$

Where $L\sigma 1n$ and $L\sigma 2n$ – inductance of phase scattering of stator and rotor windings taking into account saturation, Lm – mutual inductance. To solve the differential equations (1), we use numerical integration. From the point of view of stability of numerical integration, it is advisable to solve the differential equations (1) with respect to the flow connections of the stator and rotor windings. We introduce the notation:

$$k_{rs} = L_r/L_{ms}; \quad k_{rs} = L_s/L_{ms}; \quad k_m = L_m/L_{ms} \tag{2.6}$$

Where $L_{ms}=L_s \cdot L_r - L_m^2$ – determinant of matrix coefficients of the equation.

With the accepted notation (2.6) from equation (3.2, 3.3), we Express the currents of the stator and rotor windings:

$$\left.\begin{aligned} i_{su} &= \psi_{su} \cdot k_{rs} - \psi_{ru} \cdot k_m; \\ i_{sv} &= \psi_{sv} \cdot k_{rs} - \psi_{rv} \cdot k_m; \\ i_{ru} &= \psi_{ru} \cdot k_{sr} - \psi_{su} \cdot k_m; \\ i_{rv} &= \psi_{rv} \cdot k_{sr} - \psi_{sv} \cdot k_m. \end{aligned}\right\} \quad (2.7)$$

Substitute (2.7) in (2.1) and bring the mathematical model (2.1) to a form convenient for numerical integration:

$$\left.\begin{aligned} d\psi_{su} &= [u_{su} + \omega_x \cdot \psi_{sv} - r_s \cdot (\psi_{su} \cdot k_{rs} - \psi_{ru} \cdot k_m)] \cdot dt; \\ d\psi_{sv} &= [u_{sv} - \omega_x \cdot \psi_{su} - r_s \cdot (\psi_{sv} \cdot k_{rs} - \psi_{rv} \cdot k_m)] \cdot dt; \\ d\psi_{ru} &= [(\omega_x - \omega_r) \cdot \psi_{rv} - r_r \cdot (\psi_{ru} \cdot k_{sr} - \psi_{su} \cdot k_m)] \cdot dt; \\ d\psi_{ru} &= [(\omega_r - \omega_x) \cdot \psi_{ru} - r_r \cdot (\psi_{rv} \cdot k_{sr} - \psi_{sv} \cdot k_m)] \cdot dt. \end{aligned}\right\} \quad (2.8)$$

Voltages u_{su} and u_{sv} the stator windings are expressed in terms of the output voltage FC:

$$\left.\begin{aligned} u_{su} &= U_x \cdot \cos(\varphi_u - \varphi_k), \\ u_{sv} &= U_x \cdot \sin(\varphi_u - \varphi_k). \end{aligned}\right\} \quad (2.9)$$

The amplitude of the phase voltage *Ux* is a module representing the voltage vector of the stator winding. The amplitude of the phase voltage frequency converter, phase angle of the stress vector ϕ_u and the angle of rotation ϕ_k system of coordinate axes *u,v* relative to the a axis of the three phase stator winding are set by the initial conditions.

For scalar control FC it is advisable to set the initial conditions ϕu=0 and ϕk=0. In this case, at the moment of time *t*=0 ось *u* coordinate system *u,v* and an image of a voltage vector *Ux* directed along the axis of phase a of the three phase stator winding, in equation (2.9): $u_{su}=U_x$, u_{sv}=0. Initial conditions at a time *t*=0 set thread connections ψ_{su}, ψ_{sv}, ψ_{ru}, ψ_{rv} windings, the frequency ωr of rotation of the rotor, the frequency *fx* FC.

Under the given initial conditions, the following rotational speed is calculated at each step of numerical integration: ω_x (2.2); increment photocosplay (2.8); the flux linkage of the windings

$$\left.\begin{aligned} \psi_{su} &= \psi_{su} + d\psi_{su}, \quad \psi_{sv} = \psi_{sv} + d\psi_{sv}, \\ \psi_{ru} &= \psi_{ru} + d\psi_{ru}, \quad \psi_{rv} = \psi_{rv} + d\psi_{rv}; \end{aligned}\right\}$$

currents in the stator and rotor windings (2.7); electromagnetic moment

$$M_{эм} = \frac{m}{2} \cdot p \cdot (\psi_{su} \cdot i_{sv} - \psi_{sv} \cdot i_{su}),$$

Where m=3 – number of stator winding phases, p – the number of pairs of motor poles; the increment of the angular speed of the rotor

$$d\omega_r = p \cdot \left(\frac{M_{эм} - M_c(t)}{J_\Sigma} \right) \cdot dt;$$

the rotor speed and the current time

$$\omega_r = \omega_r + d\omega_r, \quad t = t + dt.$$

By ur currents. (7) at each step of numerical integration, we calculate: module *Is*1 representing the current vector of the stator winding

$$I_{s1} = \sqrt{i_{su}^2 + i_{sv}^2};$$

phase angle ϕ_i representing the current vector of the stator winding

$$\varphi_i = \varphi_u - \text{argtg}(i_{sv} / i_{su});$$

power factor

$$\cos\varphi_a = \cos(\varphi_i);$$

active engine power

$$P_a = \frac{m}{2} U_x I_{s1} \cos\varphi_a.$$

At start frequency-controlled asynchronous motors with maximum load moment with reduced control time *treg* and, especially with the increase in voltage compensation *Uком* (Picture 2.1) the currents in the windings can exceed the rated ones by two or more times. Frequency-controlled asynchronous motors can be performed with closed rotor slots. For such motors, at currents starting from the nominal and higher, due to saturation of the bridge with the scattering flows of the closed rotor slots, the slot scattering of the rotor winding decreases. Short-circuited winding variable frequency drive can be performed from copper [4]. The maximum upper frequency can be 100 Hz and above at a nominal frequency of f_1=50 Hz. Consequently, in the mathematical model it is advisable to provide for the effect of iron saturation of the magnetic core by scattering flows on the scattering inductance of the stator windings $L_{\sigma 1}$ and rotor $L_{\sigma 2}$, as well as the effect of current displacement in the rotor rods on the active resistance r_r rotor winding. This will allow you to model "hard" starts, in which the influence of saturation and current displacement is most relevant.

Leakage inductance considering saturation can be calculated as a function of the current of the stator winding, and the active resistance of the rotor taking into account of displacement current as a function of the frequency of the current in the rotor winding. Based on engine design data, the following are considered known: not saturated $L_{\sigma 1}$, $L_{\sigma 2}$ and rich L_{1p}, L_{2p} when sliding s=1 leakage inductance of the windings of the stator and rotor; starting current I_{p1} the stator winding and the resistance r_{2p} the rotor winding at slip s=1. To account for the effect of saturation, the difference between non-saturated and saturated values of the scattering inductors is determined

$$\Delta L_1 = L_{\sigma 1} - L_{1p}, \quad \Delta L_2 = L_{\sigma 2} - L_{2p}$$

The current function Is1 calculates the saturated values of the scattering inductors of the stator and rotor windings

$$L_{\sigma 1n} = L_{\sigma 1} - \frac{\Delta L_1 \cdot \sqrt[3]{I_{p1}}}{\sqrt[3]{I_{p1}} - \sqrt[3]{I_{kp}}} \cdot \left(1 - \frac{\sqrt[3]{1{,}41 I_{kp}}}{\sqrt[3]{I_{s1}}}\right),$$

$$L_{\sigma 2n} = L_{\sigma 2} - \frac{\Delta L_2 \cdot \sqrt[3]{I_{p1}}}{\sqrt[3]{I_{p1}} - \sqrt[3]{I_{kp}}} \cdot \left(1 - \frac{\sqrt[3]{1{,}41 I_{kp}}}{\sqrt[3]{I_{s1}}}\right),$$

Where I_{kp} – the critical current of the stator winding, below which the saturation of the magnetic circuit does not have a noticeable effect on the inductance of the windings scattering. The value of this current is determined from preliminary calculations of the mechanical characteristics of the engine. In the case of closed slots on the rotor it is advisable to accept the current I_{kp} equal to the rated current of the stator winding. To account for saturation it is sufficient to perform 3-4 consecutive approximations at each integration step.

To account for the effect of current displacement in the rotor winding rods, the slip is calculated at each integration step

$$s_x = \left(1 - \frac{\omega_r}{\omega_1}\right) \cdot \frac{f_x}{f_1}$$

and the coefficient of change of the active resistance of the rotor

$$k_{rx} = 0,2 + \left(\frac{r_{2p}}{r_2} - 0,2\right) \cdot \sqrt{\text{abs}(s_x)},$$

Where f_1 – base frequency for which the engine is designed, $\omega_1=2\pi f_1$ – angular frequency, r_2 – the resistance of the rotor winding without taking into account current displacement.

If $k_{rx}>1$, the active resistance of the rotor winding taking into account current displacement is calculated by the formula $r_r=k_{rx}.r2$, or $r_r=r_2$.

The initial data for modeling is the nominal data and parameters of the engine.

Nominal data: the nominal power of the engine P_n, rated phase voltage $U_{нф}$, network frequency f_1, number of pairs of poles p, efficiency $\eta_и$, power factor $\cos\phi$, rated slip s_n, multiplicity of starting current I_{p1}, multiplicity of starting and critical moments M_{p1}, M_{k1}, the total moment of inertia of the rotor and the mechanism driven to the motor shaft $J\Sigma$.

The motor parameters take into account the inductive and active resistances corresponding to the nominal (without taking into account the iron saturation and the current displacement of the) and starting modes of engine operation (taking into account iron saturation and current displacement during sliding s=1). Parameters of the rated operating mode: inductive resistance of the stator windings scattering $x_{\sigma 1}$ and rotor $x_{\sigma 2}$, active resistance of the stator winding rs and rotor r_r, mutual induction inductive resistance x_m, saturation coefficient of the magnetic circuit in idle mode $knas$. The parameters in the starting mode: inductive scattering resistances $x\sigma 1p$ and $x\sigma 2p$ – stator and rotor windings, active resistance of the rotor winding r_{2p}.

In the program of mathematical modeling the load moment $Mc(t)$ it is considered constant, but can be set depending on the rotor speed ω_r active, figure 2.1, a, or reactive, pic. 1, *б*.

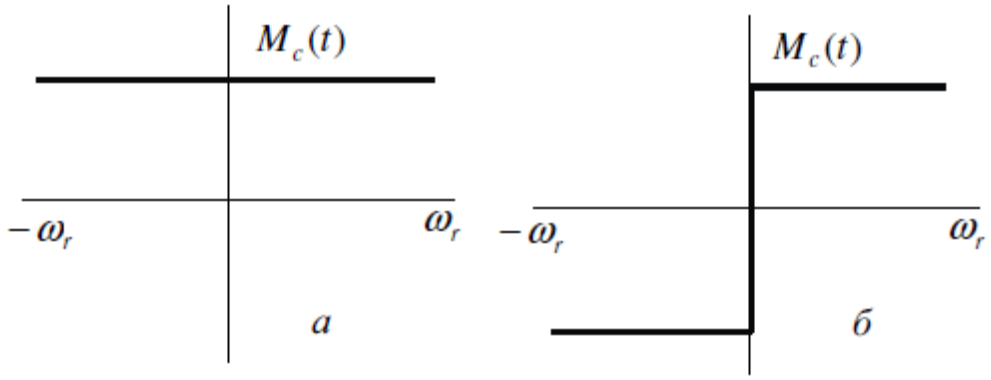

Picture 2.1 - Mechanical characteristics of the load moment

The value of the load moment is set in relative units by the coefficient $k_{mc}=M_c(t)/M_н$, where $M_н$ – rated motor torque. In the case of a reactive moment, the coefficient k_{mc} accepts the sign of the direction of the rotor speed, i.e.. $k_{mc}=k_m$csign(ωr).

The mathematical modeling program provides for the possibility of frequency control *fx* and voltage *Ux* industrial frequency according to a linear law, picture 2.6, with the compensation voltage.

Voltage and frequency industrial frequency shown in the figure 2.6 in relative units (o.e). The set values of voltage and frequency are taken as the base values of voltage and frequency.

Times are set in the source data: *treg* – regulation according to a linear law of frequency and voltage industrial frequency when the engine accelerates; *trav* – the operation of the engine at the steady state values of the frequency *fyst* and voltage U_{yst} industrial frequency; t_{ost} – stopping the engine, for which frequency and voltage FC they change according to the linear law up to their critical values *fkr* и *Ukr*.

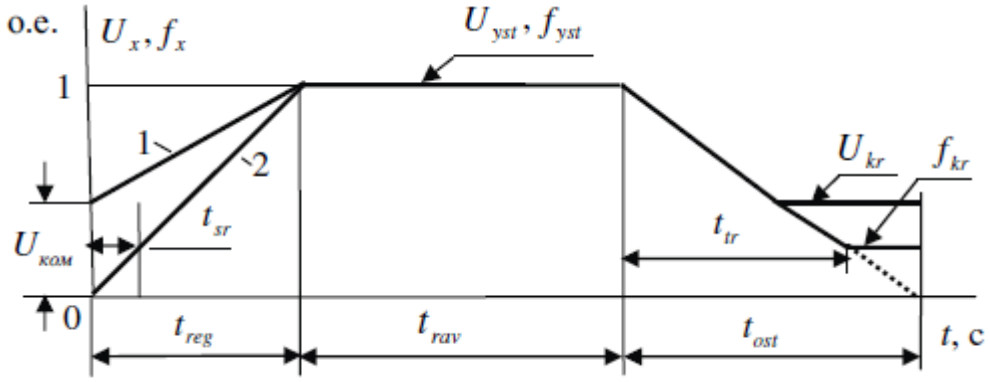

1) voltage Ux, 2) Frequency fx.

Picture 2.2 - Voltage and frequency diagrams industrial frequency:

When the load moment is active, it is set t_{sr} – the time during which the engine is stopped and after which the brake device is triggered and the engine is

released. At critical frequency values f_{kr} and voltages U_{kr} the brake device is triggered, followed by engine braking and disconnecting it from the FC.

The mathematical modeling program provides the ability to set initial parameters U_0, f_0 (при t=0) and established U_{yst}, f_{yst} voltage and frequency values FC. During regulation t_{reg} frequency and voltage industrial frequency change from the initial to the established values according to the linear law.

It is possible to set only the initial and steady frequency industrial frequency. В этом случае за время t_{reg} the frequency changes according to a linear law

$$f_x = \frac{f_{yst} - f_0}{t_{reg}} \cdot t + f_0.$$

When the condition is met $(t_{reg}+t_{rav}) \geq t \geq t_{reg}$ accepts $f_x=f_{yst}$. At time $t>(t_{reg}+t_{rav})$ the frequency also changes according to a linear law

$$f_x = f_{yst} - \frac{f_{yst}}{t_{ost}} \cdot (t - t_{reg} - t_{rav}).$$

If voltage is a function of frequency $Ux=f(fx)$ and taking into account the voltage $Uком$ compensation is calculated using the formula

$$U_x = \sqrt{2} \cdot \left(U_{ком} + \frac{U_{нф} - U_{ком}}{f_1} \cdot f_x \right),$$

where $U_{нф}$ and f_1 – rated values of the phase voltage and frequency of the motor voltage.

The brake device is activated (figure 2.6) when the engine accelerates at a time t_{sr}, when braking – at the moment of time $t>t_{tr}$. In the source data for the mathematical model of the brake device, the following parameters are set: t_{sr} – disinhibition time and $M_{тм}$ – maximum braking torque. The braking torque is a function of the time and speed of the rotor. In the time function, the brake moment from 1*kr U*1 changes over time *tsr* according to the linear law – from the maximum value to zero in the disinhibition mode and from zero to the maximum value in the braking mode.

The above model is applied to the HRAD with a short-circuited rotor with a power of 800 kW. As an example, figure 2.2 shows the simulation results. The cargo is lifted in the engine mode, and the cargo is lowered in the generator mode.

According to the technical specification the engine must provide constant torque in the frequency range from 5 to 50 Hz and constant power on the motor shaft at frequencies from 50 to 100 Hz. According to the technical specification the maximum load moment M_c=1,2$M_н$. The simulation results correspond to the load limit moment, steady-state frequency f_{yst}=5 Hz, compensation voltage $U_{ком}$=10 V,

time of regulation of voltage and frequency when starting the engine t_{reg}= 4 C, with a mechanical characteristic for one of the two engines is shown in figures 2.7 and 2.8.

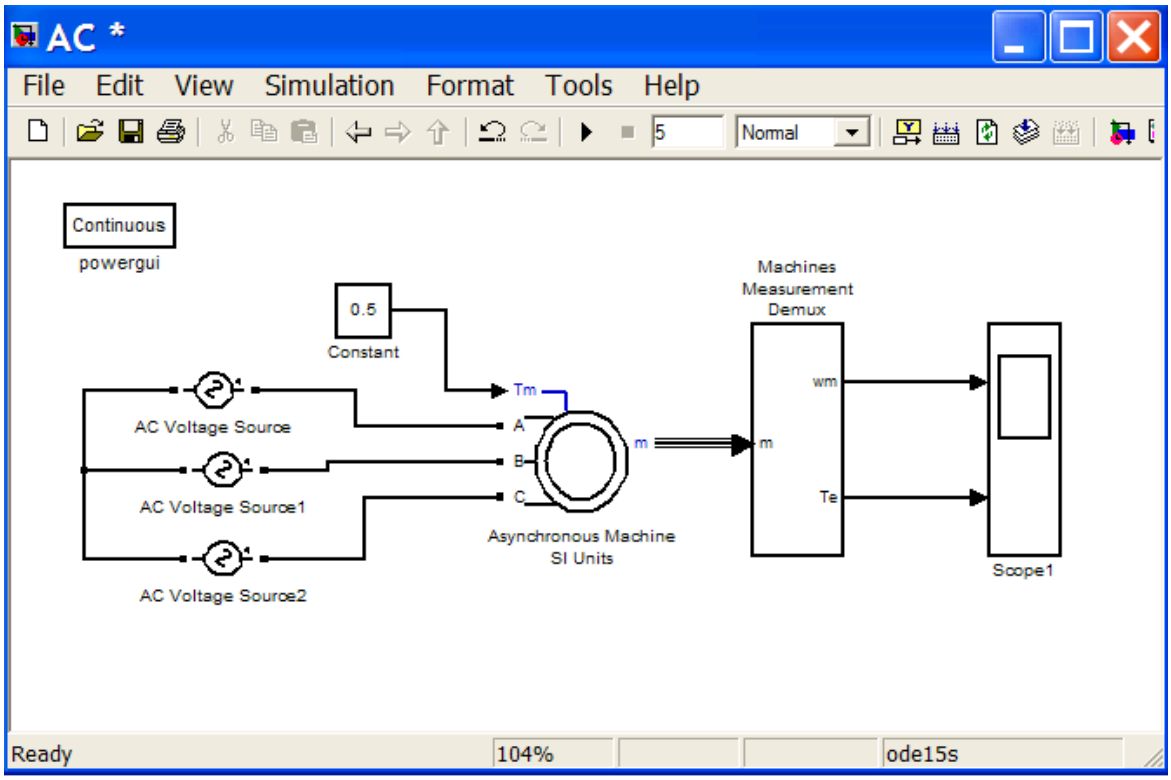

Figure 2.3-AD 1 Model for the study of transients, velocity, and electromagnetic moment

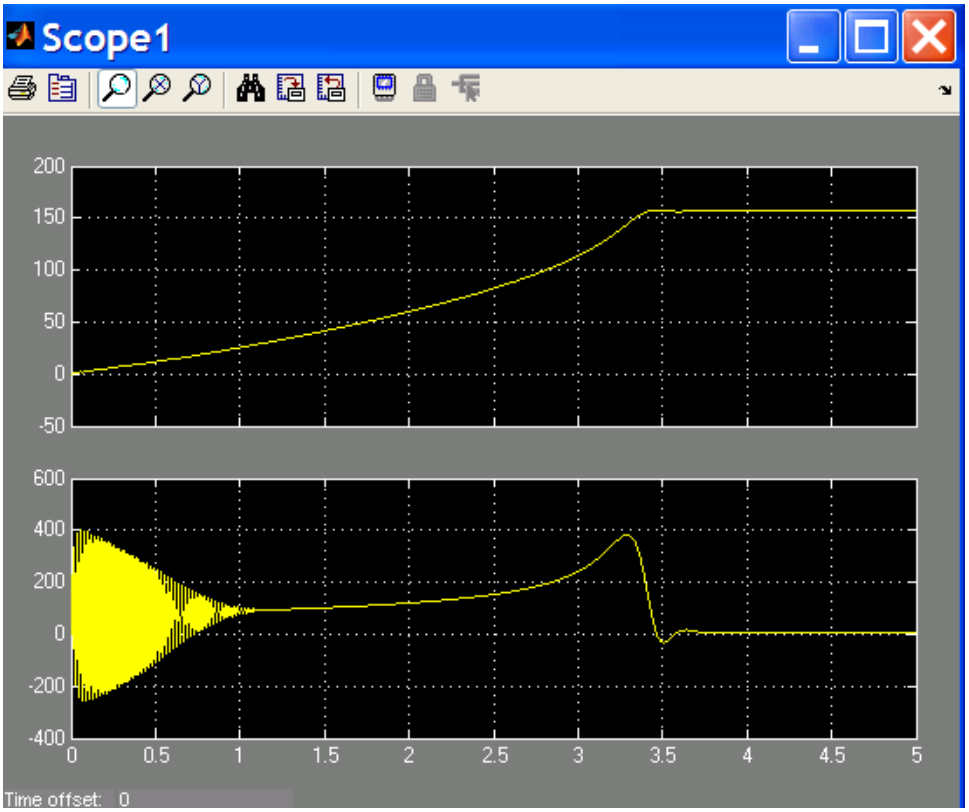

Figure 2.4 - AD Transients, speed and electromagnetic moment

Based on mathematical modeling, the following is established:

a) the Adopted law regulating the frequency and voltage of the if (at the compensation voltage $U_{ком}$=10 В) provide reliable lifting and lowering of the load by the engine in accordance with the TOR.

б) The mechanical characteristic of the brake device contributes to a uniform acceleration of the engine to a steady speed.

To solve the practical problem of the dissertation, namely, the development of control of the two-engine lift mechanism, a complex of research works is required to study the causes and dependencies of the formation of the process of uneven load distribution in mechanically interconnected multi-engine systems with frequency-controlled drives.

Research work should be carried out using mathematical modeling (MATLAB 7/Simulink).

Based on the above, the work is divided into the following stages: Determining the causes and patterns of uneven load distribution. For a detailed study of the physical principles of moment imbalance formation in a frequency-controlled electric drive in static and dynamic operating modes, it is necessary to conduct research on the constructed mathematical model of a two-motor frequency-controlled asynchronous electric drive with a vector control system and a rigid mechanical connection.

1) The Influence of gaps and elasticity on the process of uneven load distribution. In a real actuator there are elasticity and setrootpane that to simulate in a mathematical model is extremely difficult, because they do not know the real values of these quantities at the same time, the issues of gap influence on the studied process is important, and their validation is only possible on a physical object, so the data obtained in the second stage of the research, must be supplemented by results of a study of frequency-regulated electric drive on a physical model with simulated gaps and elasticities in the mechanical coupling of the drives.

2) As the basis for building a model of an unregulated two-motor asynchronous electric drive with a rigid mechanical connection, an asynchronous short-circuited electric motor was taken from the Simulink simulation program model library. In addition, there were used the basic elements from other models of the asynchronous electric drive.

According to figure 2.5, the model consists of two main parts. These are models of tested electric motors D8, D9 and a mechanical communication unit that simulates the process of total load distribution when working mechanically interconnected asynchronous motors. The principle of operation of this unit is described by well-known equations, the basic of which is the equation of the proportional distribution of moments in relation to the stiffness of mechanical characteristics, provided that the speeds of the ideal idle speed and various stiffness of mechanical characteristics are equal.

It is known that in this case, the resulting mechanical characteristic of a two-motor electric drive corresponds to.

$$\frac{M_1}{M_2} = \frac{\beta_1}{\beta_2}; \tag{2.10}$$

$$\beta = \Delta M / \Delta\omega; \tag{2.11}$$

where

ΔM – changing the moment, N·m;

$\Delta\omega$ – change in angular velocity, rad / s;

M_1, M_2 - engine torque D1 and D2, N·m;

β_1, β_2 - mechanical characteristics of the stiffness, N·m·s;

The input parameters of the block are the output values of asynchronous motor models (electromagnetic moment, currents, angular velocities, etc.) and the total set load moment for electric motors. The output values of the block are the load moments for each engine, the angular velocities and electromagnetic moments of both machines, as well as the angular velocity value of the resulting mechanical characteristic of the two-motor electric drive.

The scheme includes switches for "single-engine mode" and "multi-engine mode". This allows you to remove the data of mechanical characteristics in both modes, without making additional changes to the model. It also provides visualization of the main parameters, both the engines themselves and their power sources.

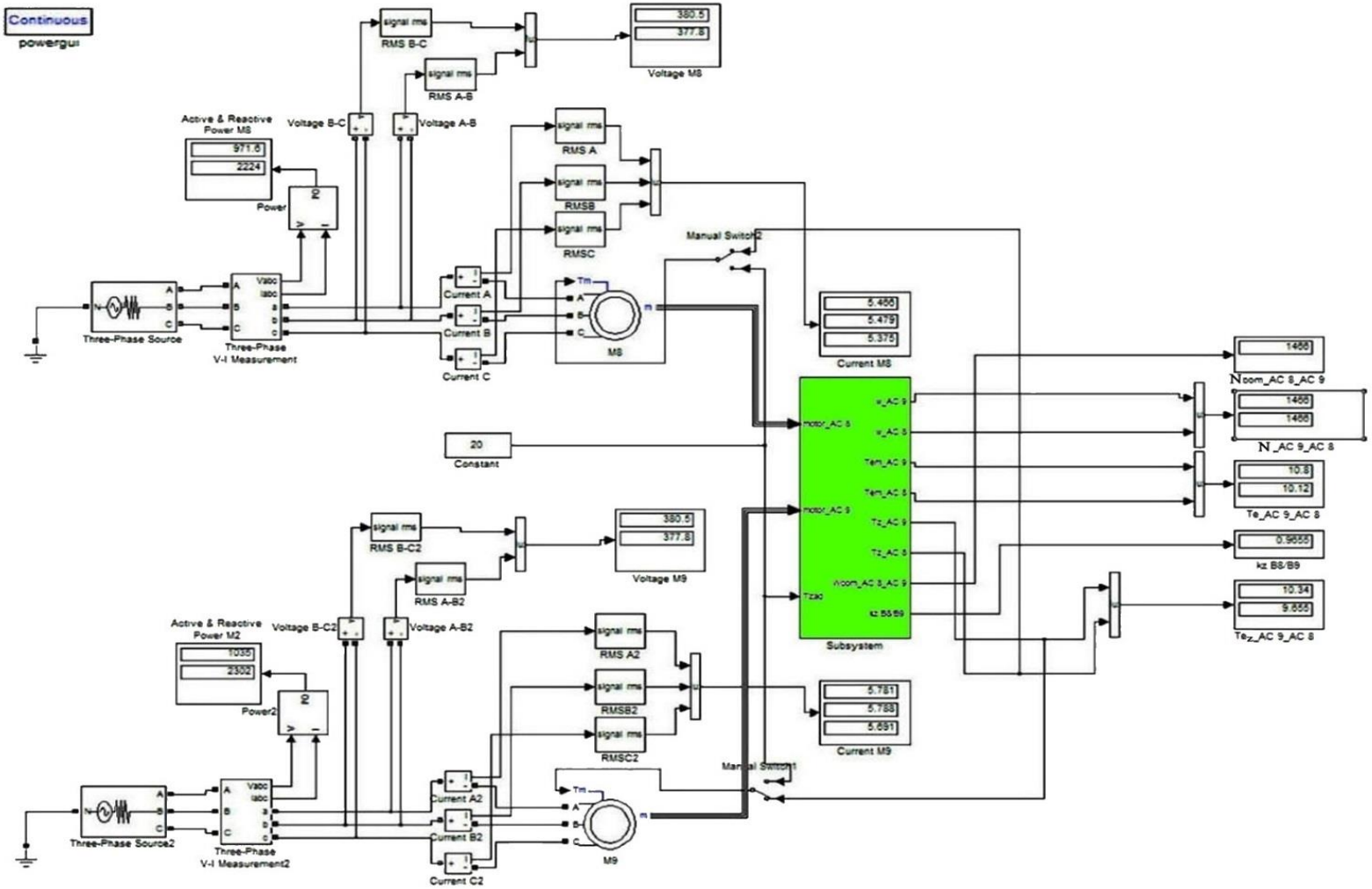

Picture 2.5 - Model SIMULINK unregulated twin-engine asynchronous electric drive with a rigid mechanical connection of the shafts

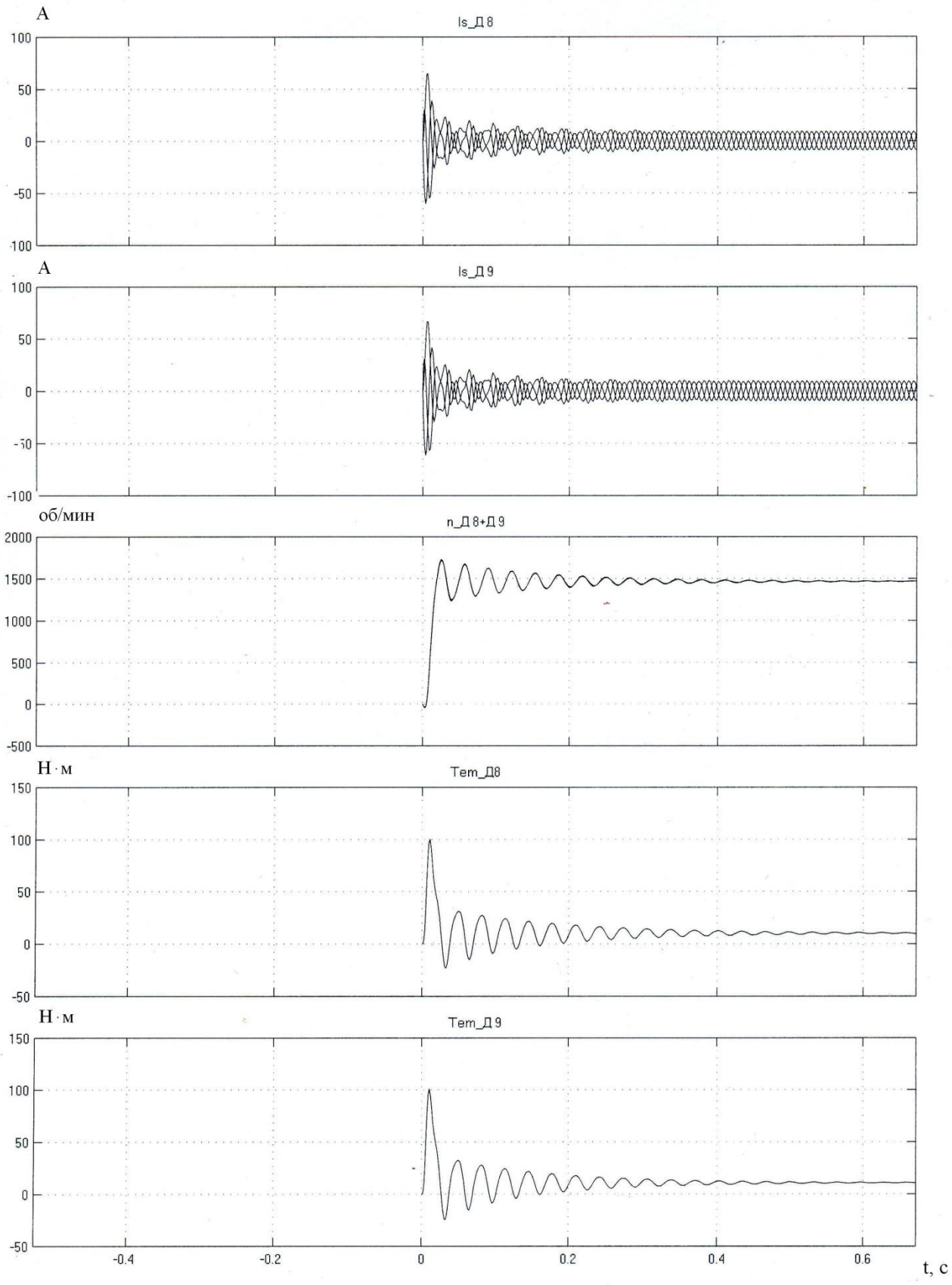

Picture 2.6 - Diagrams of currents, speeds and moments of a two-motor asynchronous electric drive with mechanical coupling obtained during experiments in Simulink.

T a b l I C a 2.1-data of mechanical characteristics obtained during testing of D8 and D9 in SIMULINK.

SIMULINK				
Engine E9				
Te_{11}=$Te_{9\ зад}$, N·m	**Te_9, N·m**	**K_9=Te_9 - $Te_{9\ зад}$**	**n_9, rpm**	**$I_{д9}$, A**
0,04	0,39	0,36	1499	5,4
1,77	2,17	0,39	1494	5,3
3,64	4,04	0,40	1488	5,4
7,36	7,75	0,39	1476	5,5
10,97	11,37	0,4	1464	5,9
14,61	15,02	0,41	1451	6,4
18,23	18,6	0,37	1438	7,1
21,90	22,3	0,4	1424	7,8
25,51	25,85	0,34	1409	8,6
29,18	29,59	0,41	1393	10,5
		K_9~0,4		
Engine E8				
Te_{11}=$Te_{8\ зад}$, N·m	**Te_8, N·m**	**K_8= Te_8- $Te_{8\ зад}$**	**n_8, rpm**	**$I_{дв8}$, A**
0,02	0,39	0,38	1499	5,1
1,81	2,20	0,39	1493	5,1
3,62	4,03	0,41	1487	5,1
7,25	7,64	0,39	1475	5,3
10,91	11,28	0,37	1462	5,7
14,55	14,96	0,41	1448	6,2
18,24	18,61	0,37	1434	6

				,9
21,86	22,3	0,43	1419	7 ,7
25,55	25,9	0,35	1403	8 ,5
29,19	29,64	0,45	1386	9 ,3
		K_8~0,4		

The results of the tests are shown in tables 2.1 and 2.2. In accordance with figure 2.6 diagram of currents, moments and speed test of the model, and for clarity and ease of comparison of information obtained during research the data of the experiments were shown in tables 2.1, 2.2 and 2.2. In accordance with the data of table 2.1 and by relations (2.1) and (2.2) defines the stiffness coefficients β8 and β9, and the load distribution ratio K_β for E8 and E9. In table 2.2 the received values are given.

Table 2.2 - Calculation of stiffness coefficients and load distribution coefficient

Changing the load and speed of the engines		
E9	**Te_9, N·m**	**ω_9, rad / s**
Minimum value	0,39	156,97
Maximum value	29,59	145,87
Δ	29,19	11,10
E8	**Te_8, N·m**	**ω_8, rad / s**
Minimum value	0,39	156,97
Maximum value	29,64	145,14
Δ	29,24	11,83
Rigidity of the mechanical characteristic		
E8 и E9	**β9=Δ Te_9/Δ ω_9, N·m·s**	**β8=Δ Te_8/Δ ω_8, N·m·s**
ΔM	29,19	29,24
Δω	11,10	11,83
β	2,6	2,5
Load distribution coefficient		

$К_β=β8/β9$	0,965

The resulting load distribution coefficient $К_β$ used in the simulation block for uneven load distribution of the simulation model.

The results of tests in the multi-motor electric drive mode are shown in table 2.2.

The adequacy of the simulation model of a two-motor unregulated asynchronous electric drive with a rigid mechanical connection was evaluated by comparing the values of output parameters in static operation, such as speed, current and torque obtained as a result of simulation and bench modeling.

In accordance with table 3.2, the discrepancy between the speed values obtained on the stand and the simulation in Simulink at the same value of the load moment varies within 2-4 rpm and does not exceed 1%.

The difference in currents on average is 0.2-0.9 A and does not exceed 10% in the range of current changes from idle to nominal value.

In addition, in accordance with figure 2.2, the speeds of both engines in dynamic and static operation are the same, which corresponds to a two-engine version of an Electromechanical system with a rigid mechanical connection.

Thus, the results obtained confirm the similarity of simulation and physical Electromechanical systems, as well as the adequacy of the model in static operation.

Therefore, the calculated values of engine torques are correct and correspond to the actual distribution of torques when operating the interconnected E8 and E9 on the total load.

Table 3.2 - Mechanical characteristic data obtained during testing E8 и E9 on the stand and in SIMULINK in the mode of a two-motor drive with a rigid

SIMULINK					
Engine E8+E9					
Te_9, N*m	**Te_8, N*m**	**$K_{8,9}= Σ Te_{8,9}- Te_{11}$**	**n,** winding/ minutes	**$I_{дв9}$, A**	**$I_{дв8}$, A**
0,45	0,45	0,81	1499	5,4	5,1
1,32	1,26	0,82	1496	5,3	5,05
2,28	2,15	0,82	1493	5,3	5,05
4,18	3,93	0,82	1487	5,4	5,1
6,08	5,70	0,79	1481	5,4	5,2
7,94	7,44	0,80	1475	5,6	5,3
9,79	9,17	0,77	1469	5,7	5,4
11,7	10,94	0,75	1463	6,0	5,7
13,6	12,73	0,79	1456	6,2	5,9
15,52	14,52	1,51	1448	6,5	6,1

19,26	18,01	0,78	1436	7,2	6,7
22,98	21,48	0,74	1421	7,9	7,5
26,73	24,97	0,72	1406	8,8	8,3
		$K_{8,9}$~0,8			

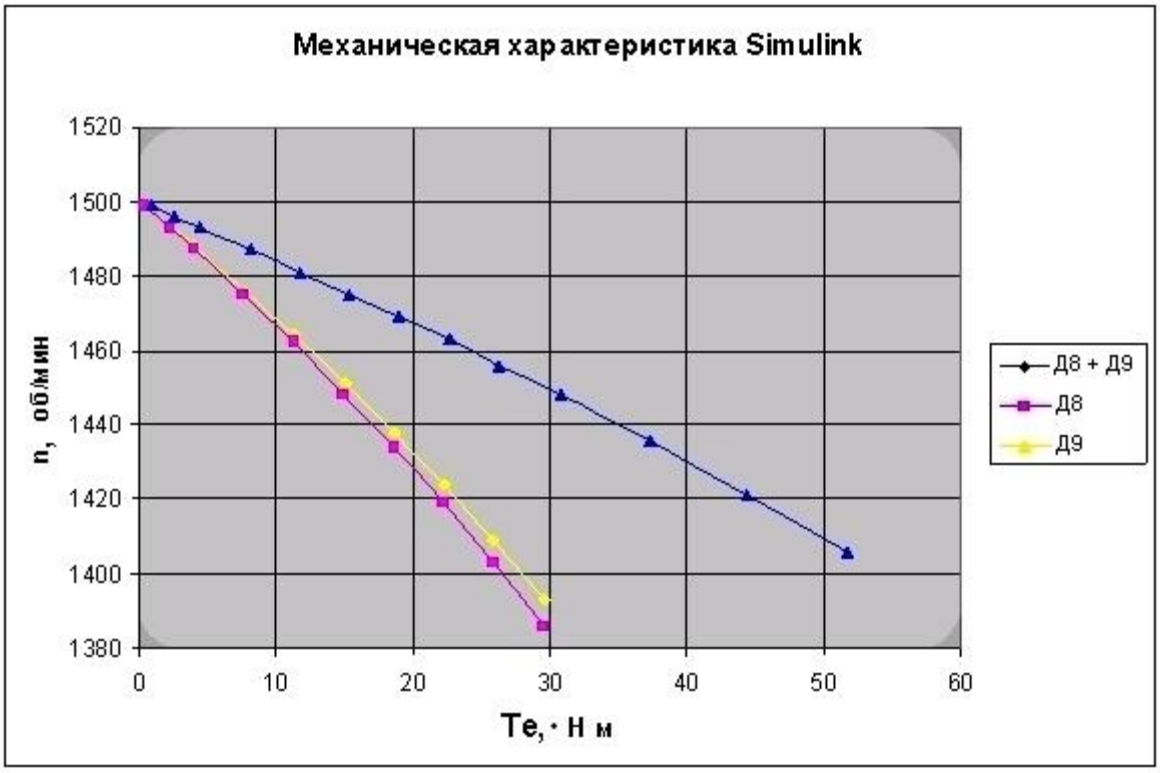

Picture 2.7 - Graphs of mechanical characteristics based on data obtained during experiments

2.1 Determination of the causes of the moment imbalance in an electric drive with a rigid mechanical connection

A mathematical model of a two-motor asynchronous electric drive with a vector control system and rigid mechanical coupling has been developed for a detailed study of the causes and physical principles of moment imbalance formation in a vector-controlled electric drive in static and dynamic operating modes. Models of frequency converters with a vector control system are used as the basis Simulink (F.O.C.).

The basic equations describing the operation of blocks of the asynchronous drive simulation model with a vector SU are given below (F.O.C.):

$$\Theta_e = \int \left(\omega_r + \Delta\omega_{si} \right) \cdot dt \tag{2.12}$$

where Θ_e – instantaneous value of the electric angle of rotation of the x-y coordinate axes relative to a fixed coordinate system α-β;

ω_r – angular electric speed of rotation of the rotor, rad / s;

$\Delta\omega_{si}$ – slip calculated from iqs and engine parameters, rad / s;.

$$\left|\Psi_r\right| = \frac{L_m \cdot i_{ds}}{1 + \tau_r \cdot s} \tag{2.13}$$

where Ψ_r – modulus of the rotor flow coupling vector;

τ_r - electromagnetic time constant of the rotor circuit;

L_m – mutual induction of windings, mgN;

i_{ds} – the component of the stator current that provides the formation of flow coupling, And.

$$\begin{aligned} V_d &= \frac{2}{3}\left(V_a \sin(\omega t) + V_b \sin\left(\omega t - \frac{2\pi}{3}\right) + V_c \sin\left(\omega t + \frac{2\pi}{3}\right)\right); \\ V_q &= \frac{2}{3}\left(V_a \cos(\omega t) + V_b \cos\left(\omega t - \frac{2\pi}{3}\right) + V_c \cos\left(\omega t + \frac{2\pi}{3}\right)\right); \\ V_0 &= \frac{1}{3}(V_a + V_b + V_c). \end{aligned} \tag{2.14}$$

$$\begin{aligned} V_a &= V_d \sin(\omega t) + V_q \cos(\omega t) + V_0; \\ V_b &= V_d \sin\left(\omega t - \frac{2\pi}{3}\right) + V_q \cos\left(\omega t - \frac{2\pi}{3}\right) + V_0; \\ V_c &= V_d \sin\left(\omega t + \frac{2\pi}{3}\right) + V_q \cos\left(\omega t + \frac{2\pi}{3}\right) + V_0. \end{aligned} \tag{2.15}$$

where $abc \square \quad dq$ – conversion from three-phase system signals V_a, V_b, V_c, into a two-phase rotating coordinate system V_d, V_q, V_0 and vice versa.

$$i_{qs}^* = \frac{2}{3} \cdot \frac{2}{p} \cdot \frac{L_r}{L_m} \cdot \frac{T_e^*}{\left|\Psi_r\right|} \tag{2.16}$$

$$i_{ds}^* = \frac{\left|\Psi_r\right|^*}{L_m} \tag{2.17}$$

where I_{qs}, I_{ds} – components of the stator current that provide the formation of the moment and flow coupling, A;

L_r – the inductance of the rotor, RH;

T_e^* - set motor electromagnetic moment, N·m.

Mechanical communication is implemented by combining data from a mechanical system that is part of the engine model and allows you to reproduce the dynamics of an electric machine, depending on the selected channel for setting the moment or speed, with a library model of a mechanical shaft (MSB) that simulates the relationship between the drive motor and the load. The equations describing how the block works are shown below:

$$T_e = J\frac{d}{dt}\omega_r + F\omega_r + T_m; \tag{2.18}$$

$$T_{sh} = K_{sh}\int(\omega_r - \omega_l)dt + D_{sh}(\omega_r - \omega_l). \tag{2.19}$$

where T_e – motor electromagnetic torque, N·m;
T_{sh} – transmitted torque N·m;
J- total moment of inertia, kg * m2;
T_m- load moment on the motor shaft, N·m;
F – total coefficient of viscous friction for the rotor and load;
K_{sh} – the stiffness coefficient of the shaft;
B - damping factor;
ω_r – angular rotation speed of the rotor (drive side), rad / s;
ω_l – angular rotation speed of the rotor (drive side), rad / s.

Simulink model of a frequency-controlled two-motor asynchronous electric drive with a rigid mechanical connection**.** In accordance with figure 2.5, the structure of the mathematical model formed in this way is presented. In accordance with figure 2.6 on the basis of the resulting structure was assembled in MATLAB 7/ Simulink model with a configuration of a two-motor frequency-controlled asynchronous electric drive with a rigid mechanical connection. To debug the resulting system, we used data from the parameters of the substitution schemes obtained during the first stage of research, and the real values of the parameters of the settings of frequency converters.

Research on Simulink models of uneven load distribution process**.**

The most obvious and dangerous mode of cargo descent simulation was used as the simulated process.

As a result of Simulink simulations, and in accordance with figure 2.8 and table 3.3, the two-engine system is divided into " pulling» E8 and the "driven" E9 drive. The total shaft torque generated by the load drive is 11 N·m (~ 27% of the rated total torque of the tested engines) at a given speed of 300 rpm, or otherwise 20% of the rated speed. The discrepancy of moments reaches 37.62% in dynamics and 50.8% in statics.

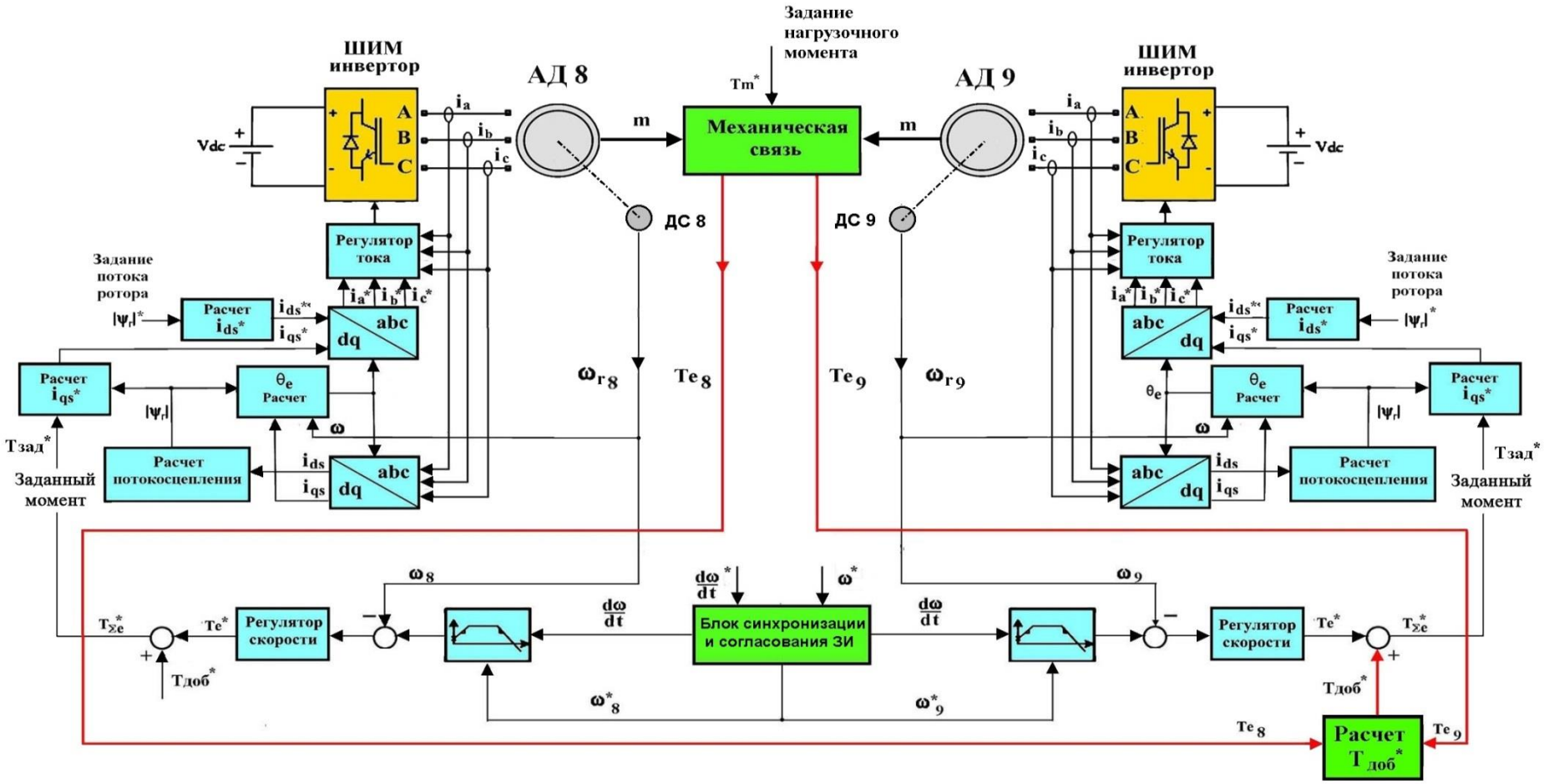

Figure 2.8-Block diagram of a mathematical model of a two-motor mechanically interconnected asynchronous electric drive with vector

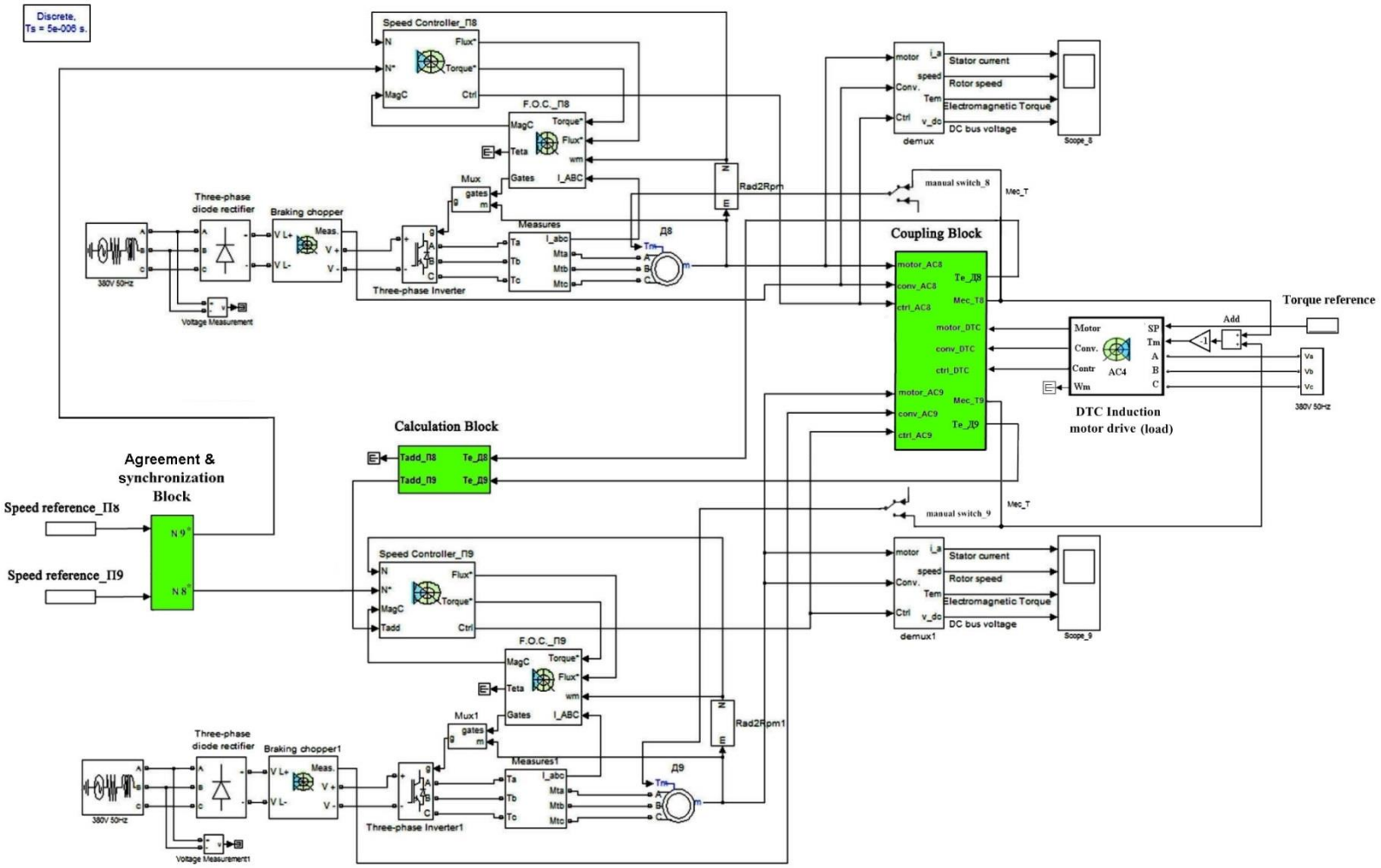

Figure 2.9-SIMULINK Model of a two-motor mechanically interconnected asynchronous electric drive with vector control

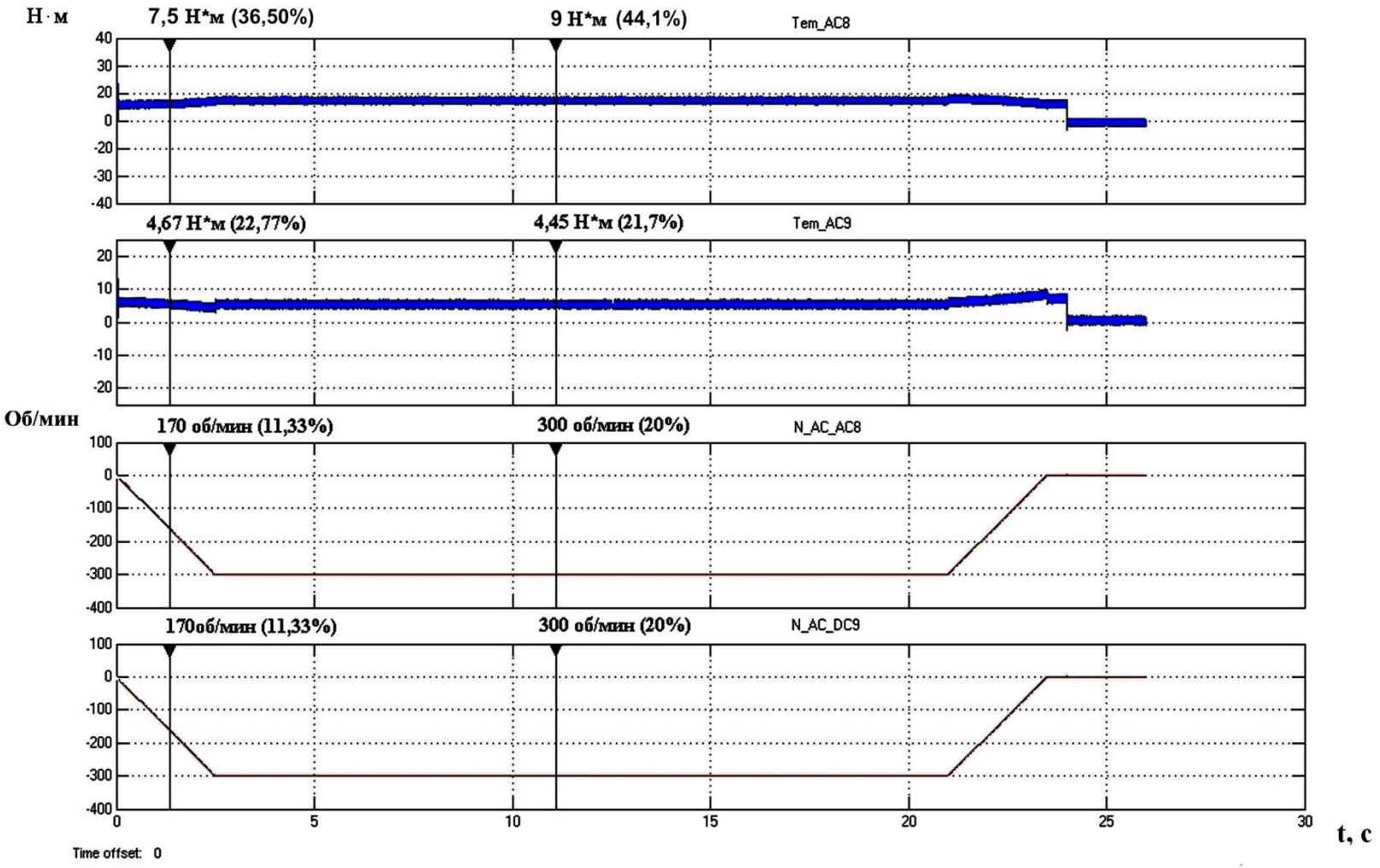

Figure 2.10 - SIMULINK uneven distribution of the total load with a rigid mechanical connection in the mode of simulated
cargodescent

The moment imbalance reaches 38.40% in dynamics and 50.01% in static.

T a b l I C a 3.3-Confirmation of the adequacy of the simulation Simulink model

Engine	Dynamic			Statics		
	moment engine, N·m	output current, A	actions'. speed, rpm	moment engine, N·m	output current, A	actions'. speed, rpm
Simulink						
E8	7,50	4,41	170	9,0	4,59	300
E9	4,67	3,98	170	4,45	4,00	300
Δ%	37,62	10,0	-	50,8	12,87	-

The adequacy of the developed model was evaluated by comparing the values of output parameters in static and dynamic modes of operation. Parameters such as speed, current, and torque obtained from simulation and similar bench experiments were used.

In accordance with table 3.4, the results obtained do not exceed 10% of the discrepancy and confirm the similarity of the simulation and physical Electromechanical systems, as well as the adequacy of the model in dynamic and static operation.

To change the settings. Further experiments were carried out on the model with changing the values of parameters settings of converters and parameters of motor substitution schemes.

1) Analysis of the obtained results allows us to determine the following reasons for misalignment in the distribution of the total load moment (including switching to generator mode):

2) non-Identity and non-synchronization of the control parameters set during the transition process;

3) availability of speed feedback.

The physical element of the control SYSTEM responsible for these reasons is the intensity setter for the speed control loop. ZI blocks form a linear rate of change in the drive control signal over time, depending on the set parameters of the transition process, namely, the acceleration-deceleration setting, speed control settings, restrictions, etc. Identical settings of frequency converters with non-identical parameters of substitution schemes of engine models form almost identical transients with a minimum value of the moment imbalance, which can be ignored in practice. But at different set acceleration rates or asynchronous feed to the input of THE zi speed setting, the drive system is divided into" pulling "and" driven " parts. In this case, the drive, which zi forms a tachogram of acceleration with a higher acceleration rate, takes on most of the load, and with a more significant misalignment of the set parameters due to the influence of the OS, the "slave" drive

switches to generator mode. This separation is formed during the transition process and persists after entering the static section of the drive operation.

In order to verify the above assumptions, an additional synchronization block was added to the simulation and physical models with a rigid mechanical connection of engine shafts. As a result, in dynamic and static modes of operation, a proportional distribution of moments was formed, the imbalance of which does not exceed 2-3%

The simulation results confirmed the above conclusions.

2.2 Influence of gaps and elasticity on the process of uneven load distribution

To verify the results of the simulation, the model was again applied with the previous configuration, corresponding to a two-motor frequency-controlled asynchronous electric drive with vector control and installation on the shafts of gear motors with the ability to regulate gap formation. Zi synchronization was performed due to a common speed setting source for both converters.

In the course of experiments, the formation of a significant imbalance and frequent transition to the generator mode continues to be observed. Analysis of the results revealed the following additional factors that can disrupt the moment balancing in both dynamic and static modes of operation. This is vibration caused by uneven gear travel, gap formation, defects, wear, elasticity, etc., impacts at the time of unregulated gap selection or non-identical rate of smoothing, as well as fluctuations in the specified load moment.

In the course of research, additional features were established in the operation of a two-motor frequency-controlled drive with a gear mechanical connection:

1)Large compared to unmanaged asynchronous electric drive amplitude of mechanical oscillations and vibrations, due to the presence of gears and the influence of the OS on a working drive system as a whole;

2) In contrast to the previously considered unregulated electric drive, in a system with vector control, when the maximum torque limit of the motor of one of the drives is reached, the moments between the drives are self-equalized, due to the compensation of sliding by a less loaded drive. In accordance with the data in table 3.5, as an example, we can give the division of the Electromechanical system into the pulling P8 and the driven part of P9 with the transition of the driven drive to the generator mode; the P8 generates an electromagnetic moment and a current close to the specified limit (rotation speed of 1500 rpm). In this case, this drive begins to "pull" not only the entire load moment, but also the generator resistance moment formed by P9. When the Tnagr reaches ~ 22 N·m, the P8 reaches the specified current limit of 7.7 A, and the SU P8 limits the further growth of the current, and therefore the motor torque. To compensate for the slip caused by a further increase in the SU load, the P9 begins to form the appropriate moment, thereby transferring the drive from the generator mode to the motor mode. Further, at a Tnagr of~38

N·m (92.5% of the nominal total torque of the tested engines), both torques and currents are equalized for both engines.

Table 2.5 - Distribution of currents and moments when changing $T_{нагр}$ from 0 to 38 N·m

$T_{нагр,}$, N·m	Te $_8$ N·m	Te $_9$, N·m	$I_{дв8}$, N·m	$I_{дв9}$, N·m
0	8,96	-8,14	5,06	4,80
1,83	19,36	-15,91	7,91	6,55
3,72	18,27	-13,25	7,43	5,92
7,37	19,35	-10,34	7,62	5,36
10,96	19,54	-7,032	7,58	4,75
14,54	19,28	-3,79	7,62	4,28
18,24	19,14	-0,12	7,57	4,15
21,87	19,52	3,22	7,77	4,25
25,54	19,30	6,82	7,92	4,65
29,16	18,79	10,50	7,69	5,39
36,46	19,20	17,99	7,71	7,10
38,05	19,31	19,37	7,53	7,33

The process of load distribution and the amount of imbalance, in contrast to an unregulated drive, are random, because they depend on the setting of the SU Converter and a number of additional effects of a random nature, and not on the run-up of the mechanical characteristics of the engines. In addition, after repeated automatic configuration, the "master-slave" status changes depending on the settings. To confirm this conclusion, two series of studies were conducted on the model, consisting of 8 experiments with 10 test launches each. With a single load moment value and a specified rotation speed of 1500 rpm. In each subsequent experiment, the load moment increased from 0 to ~36.5 N·m (85% of the nominal total torque of the tested engines). In this case, the first four experiments were performed with a single setting of the Converter, and the second four after repeated automatic configuration.

Table 2.6 – Distribution of currents and moments between D8 and D9 at initial and repeated automatic adjustment of converters and change of Tnagr from 0 to ~36.5 N·m

Initial configuration of the Converter							Re-configuring the Converter						
time=19800ms; load ~0% of the total torque of both engines							time=19800ms; load ~0% of the total torque of both engines						
Te_8, N*m	n8, rpm	$I_{дв8}$,A	Te_9 N*m	n9, rpm	$I_{дв9}$,A		Te_8, N*m	n_8, rpm	$I_{дв8}$, A	Te_9, N*m	n_9, rpm	$I_{дв9}$, A	
-6,17	1502,7	4,34	8,035	1515,5	4,94		13,40	1485	6,08	-12,17	1497,5	5,74	
-6,06	1500,5	4,27	8,25	1505,5	4,94		24,00	1497,3	8,99	-22,31	1455,15	8,32	
1,82	1487,5	3,99	-0,84	1493,5	4,17		21,98	1508,7	8,50	-20,19	1494,5	7,82	
5,08	1498,5	4,36	-3,74	1502,4	4,31		14,40	1499,4	6,37	-12,99	1513,8	5,88	
2,60	1493,5	4,06	-1,59	1500,4	4,16		25,05	1494,5	9,33	-23,11	1515,5	8,46	
-9,33	1483,5	4,98	11,94	1518,5	5,73		17,48	1508,7	7,28	-15,74	1520,7	6,60	
-13,44	1508,7	5,97	16,58	1498,5	6,70		27,54	1509,5	10,03	-25,78	1518,5	9,25	
-9,39	1472,7	4,93	12,21	1513,5	5,75		26,27	1507,5	9,53	-23,65	1517,7	8,62	
time=19800ms; load ~17% from sum moment both engines							time=19800ms; load ~17% from sum moment both engines						
Te_{11}, N*m	Te_8, N*m	n_8, rpm	$I_{дв8}$, A	Te_9, N*m	n_9, N*m	$I_{дв9}$, A	Te_{11}, N*m	Te_8, N*m	n_8, rpm	$I_{дв8}$,A	Te_9, N*m	n_9, rpm	$I_{дв9}$, A
7,29	-5,37	1490,5	4,11	15,08	1491,3	6,40	7,29	30,00	1490,5	11,10	-21,32	1502,4	8,05
7,52	6,68	1500,4	4,62	1,77	1509,4	4,18	7,36	15,28	1505,5	6,64	-6,57	1496,5	4,75
7,36	4,59	1506,4	4,30	4,10	1495,2	4,37	7,20	11,84	1509,6	5,70	-3,34	1479	4,28
7,25	-3,85	1507,5	3,94	13,43	1511,7	5,99	7,45	27,67	1526,5	10,07	-18,67	1490,5	7,29
7,68	-1,24	1500,4	3,83	10,21	1499,4	5,33	7,04	18,43	1494,5	7,62	-9,40	1493,5	5,28
7,48	-3,30	1496,5	3,9	12,65	1525,5	5,84	7,24	22,46	1477,5	8,54	-13,32	1510,5	6,03
7,30	-4,99	1503,4	4,17	14,84	1500,4	6,35	7,25	24,26	1511,7	9,07	-14,82	1489,2	6,32

Continuing table 2.6

Initial configuration of the Converter							Initial configuration of the Converter						
time=19800ms; ; load ~53% from sum moment both engines							time=19800ms; load ~53% from sum moment both engines						
Te_{11}, N*m	Te_8, N*m	n_8, , rpm	$I_{дв8}$,A	Te_9, N*m	n_9, , rpm	$I_{дв9}$, A	Te_{11}, N*m	Te_8, N*m	n_8, rpm	$I_{дв8}$, A	Te_9, N*m	n_9, , rpm	$I_{дв9}$, A
21,71	0,06	1477,5	3,91	23,20	1540,2	0,87	21,78	30,93	1473,7	11,49	-8,92	1504,5	4,97
21,92	8,55	1494,3	5,05	14,36	1513,5	6,24	21,69	22,35	1519,8	8,51	-0,26	1512,6	4,16
21,99	6,46	1473,7	4,60	16,49	1479	6,78	21,78	26,49	1509,6	9,63	-3,35	1506,4	4,28
21,94	4,43	1489,2	4,30	18,40	1479,4	7,29	21,74	29,90	1498,5	11,07	-7,69	1510,5	4,83
21,78	12,30	1514,7	5,85	10,46	1490,5	5,32	21,87	28,11	1503,6	10,16	-5,46	1491,4	4,52
21,85	-1,16	1518,7	3,86	24,86	1473,5	8,88	21,71	25,34	1477,5	9,37	-2,61	1497,4	4,24
21,83	1,72	1519,8	3,99	21,53	1519,8	8,04	21,98	17,48	1502,4	7,19	5,19	1473,5	4,54
21,95	-0,76	1483,9	3,86	24,20	1509,6	8,79	22,03	21,26	1501,5	8,17	1,26	1482	4,22
time=19800ms; load ~87% from sum moment both engines							time=19800ms; load ~87% from sum moment both engines						
Te_{11}, N*m	Te_8, N*m	n_8, , rpm	$I_{дв8}$, A	Te_9, N*m	n_9, , rpm	$I_{дв9}$, A	Te_{11}, N*m	Te_8, N*m	n_8, , rpm	$I_{дв8}$, A	Te_9, N*m	n_9, , rpm	$I_{дв9}$, A
36,46	16,09	1526,8	6,79	21,12	1502,4	7,92	36,44	30,73	1516,8	11,35	6,00	1508,5	4,59
36,52	14,34	1486,3	6,42	22,95	1510,5	8,40	36,50	30,15	1504,6	11,23	6,24	1513,6	4,63
36,41	17,53	1478,1	7,25	19,79	1512,6	7,54	36,42	30,31	1500,5	11,10	6,41	1512,6	4,78
36,31	15,08	1522,8	6,48	22,55	1491,3	8,28	36,31	29,98	1498,8	10,67	6,22	1491,3	4,60
36,39	12,78	1478,4	6,03	24,44	1518,7	8,98	36,40	31,65	1504,4	11,02	4,64	1518,7	3,98
36,69	5,34	1501,5	4,38	32,50	1508,7	11,29	36,67	35,21	1487,8	11,07	1,35	1508,7	2,78
36,60	8,91	1504,5	5,11	28,69	1501,5	10,15	36, 61	29,78	1501,4	9,82	7,32	1501,5	5,11
36,59	12,40	1514,7	5,79	25,15	1503,4	8,95	36,58	30,54	1498,5	10,95	6,20	1503,4	4,48
36,48	11,90	1502,7	5,68	25,96	1501,5	9,36	36,45	30,24	1514,3	11,42	6,52	1501,5	4,80

2.3 Upgrade of the lift control system

To modernize the SU lifting system it is necessary to develop and adjust a system for equalizing static and dynamic loads in the presence of elastic connections and gaps in the Electromechanical system based on the results of previous research stages.

When upgrading or designing a new lift with a modern frequency-controlled drive, it is necessary to take into account the high requirements for the safety and reliability of this mechanism. It is necessary to carefully analyze the features of the equipment under consideration, and the possibility of using widely used technical solutions for modernization, one of which, for example, is the load balancing system-SVN, because their inherent versatility does not always take into account the design and technological specifics of this particular equipment.

For example, on cranes of classic projects with a relay drive control system, both drives are independent of each other and are connected only mechanically by means of gears. In this case, due to the ratchet mechanism (if the electric motor is jammed or fails) and the reserve power reserve remaining in the engagement of the drive, the load is slowed and held by the crane's brake system or, if possible, at a reduced speed, the load is lowered to zero.

In a similar case, the design and use of a load balancing system for the lift mechanism based on a standard technical solution using master-slave technology will lead to a situation where the engine that remains engaged will not be able to develop sufficient torque to hold or move the working load. This is due to the fact that when the master drive shaft breaks, the slave drive control system operating in DTC mode receives a minimum value of the set torque equal to the idle speed of the asynchronous motor of the master drive.

The solution offered by the developers of SIMOVERT MASTERDIRVES VC drives from Siemens is to switch between the vector speed control mode and the vector torque control mode during operation. This function should ensure that when the mechanical connection is broken, the slave drive is switched to master mode, thus avoiding the possibility of uncontrolled control mode, which in turn implies additional measures for measuring and monitoring the torques of both engines.

The implementation of this solution by installing additional torque measuring devices on the engine shaft will require accurate and reliable installation, trouble-free operation in high temperatures, aggressive environments and high vibration, typical for the operation of load-lifting mechanisms, as well as the introduction of additional tracking circuits in the drive SYSTEM. However, the known methods of hardware and software monitoring, determining the emergency status and switching the slave drive to the master mode, to eliminate uncontrolled control mode, complicate the control system and do not provide guaranteed operation without failures and false positives at all stages of the technological process. Thus, such measures, while complicating the SU, nevertheless do not provide guaranteed reliability.

Thus, taking into account the structural and technological specifics of the casting crane, as well as high requirements for the safety of its operation, special requirements are imposed on the crane's SVN. Namely, the proportional distribution of the total moment in all operating modes and guaranteed safe completion of work when the mechanical connection is opened at any part of the trajectory of the electric drive (static section or transition stage of movement).

2.4 Development and verification of the lead-to-lead voltage recovery rate on the model

Thus, based on the results of the analysis and data from previous research stages, it can be concluded that the concept of the future lead-to-lead voltage recovery rate should be based on the principle of independent control and management of each drive (vector speed control mode for both drives). In this case, the operation of both drives must be coordinated and balanced due to the presence of an additional matching loop and a block of the torque equalization system.

In this case, both drives operate in the " lead-to-lead voltage recovery rate "lead-to-lead" mode and it does not matter when and where the mechanical connection will be broken, because the engine that remains engaged, due to the emergency power reserve, takes over the entire load and completes the technological cycle without an accident, or smoothly reduces the speed of lowering the skip to a minimum, thus avoiding unmanageable acceleration and providing the crane brake system with comfortable conditions for fixing and holding the load, while not requiring intervention in the operation of the Converter control system to switch from one control mode to another, which reduces the risk of failure at the time of an accident when working with a rated load and at maximum speed.

Thus, this solution allows you to avoid uncontrolled acceleration and critical heating of the pads, followed by slippage on the brake pulleys when closing the brakes at high speeds, and therefore achieve the required safety and eliminate the main drawback of the SVN "master-slave".

The principle of operation of the proposed unit the rate of voltage recovery is based on the calculation and introduction of corrective changes in the process of forming the value of the total output torque of one of the drives. At the same time, in a mechanically interconnected system, the regulated change in the output torque of the lift will directly affect the moment of the other drive-lift 2, thereby compensating for the existing imbalance.

The contour for calculating the implemented SVN in accordance with the drawing has a simple algorithm for calculating the correction task.

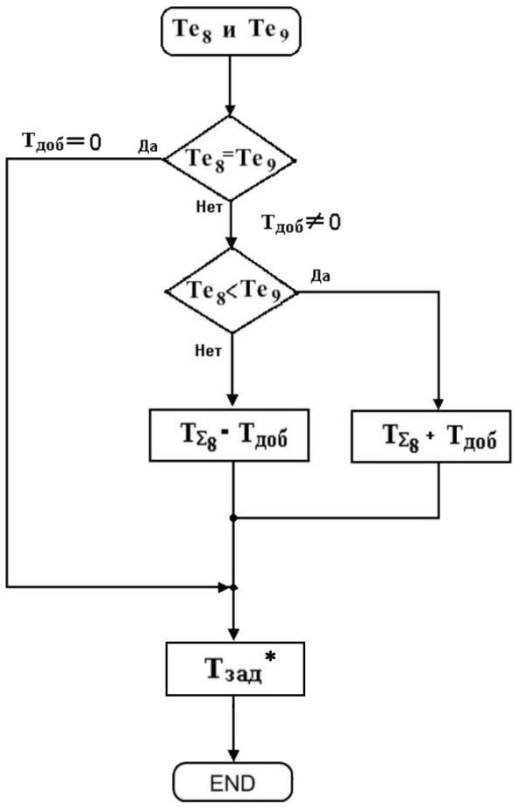

Te $_8$ and Te $_9$ – moment engine E1 and E2; $T_{доп}$ – additional corrective moment value; $T_{\Sigma 8}$ – total specified value of the moment E8; $T_{зад}^{*}$ - the specified value of the moment.

Picture 2.11 - The algorithm of the rate of voltage recovery

If Te $_8 \neq$ Te $_9$, then, accordingly, the corrective task of the moment will be $T_{доб} \neq 0$. When the condition is met Te $_8 >$ Te $_9$, meaning $T_{доб}$ deducted from $T_{\Sigma 8}$, thus reducing the drive torque E_8, If Te $_8 <$ Te $_9$, то $T_{доб}$, on the contrary, it is summed with $T_{\Sigma 8}$ by raising or lowering the output torque value until the load balance is reached Te $_8$=Te $_9$, wherein $T_{доб}=0$.

Further, for the design and debugging of the proposed scheme, the simulation model of the second stage of research was again used with THE use of the svn "lead-lead" without additional zi approval blocks.

Both drives operate in vector control mode with negative speed feedback. As a result of simulation conducted in Simulink, and in accordance with figure 4.3, there is a consistent operation of the two-motor system with a proportional division of the total torque between the drives E8 and E9. At a speed of 300 rpm (20% of the nominal speed value) and the load moment $M_{нагр}$ 11 N·m (~27% of the nominal total torque of the tested engines), the moment imbalance in dynamic and static mode does not exceed 2%, while the difference in dynamics is 1.77% and 1.33% in static.

In the course of the experiment, an emergency mode simulation was also performed with a break in the mechanical connection of the E8 engine. At the same

time, after the "break", the moment of the P8 corresponds to the idling of the engine and the sign of the moment changes to negative-0, 57 N·m, and the E9 became equal to 12.53 N·m.

After the mechanical connection is broken, the D9 engine of the P9 drive, which remains engaged, takes over the entire load and maintains the set speed of 20% without switching the system to emergency mode.

Thus, the obtained test results of the simulation model confirmed the performance of the rate of voltage recovery "lead-lead" (the discrepancy of moments does not exceed 2% in static and dynamic), including in emergency modes when simulating a break in the mechanical connection**.**

Hardware and software implementation of the rate of voltage recovery "lead-lead". In accordance with Appendix B, the analysis of the SIMOVERT MASTERDRIVES VC functional control scheme has shown that the most optimal technical solution is where the required system is built using the channel for additional setting of the moment of the Tsad in the SU of this type of frequency Converter, as well as additional service functions, namely freely programmable blocks with BICO data processing and transmission technology . The data required for this calculation, i.e. the moment P2, is transmitted between the converters over a fiber-optic or analog channel.

This solution allows you to implement an effective scheme the rate of voltage recovery for the considered type of lifting mechanisms without additional costs for upgrading the Electromechanical system of the crane and its SU. The output values of moments are taken as variable values for calculating the additional moment setting Te_8 and Te_9 both converters and as digital or analog signals are sent via SIMULINK communication modules or directly via analog channels CUVC (control Board) of the converters to the corresponding calculation block (made as an external control controller or programmatically using freely programmable blocks in one of the converters). Then the difference between these values is calculated ΔT.

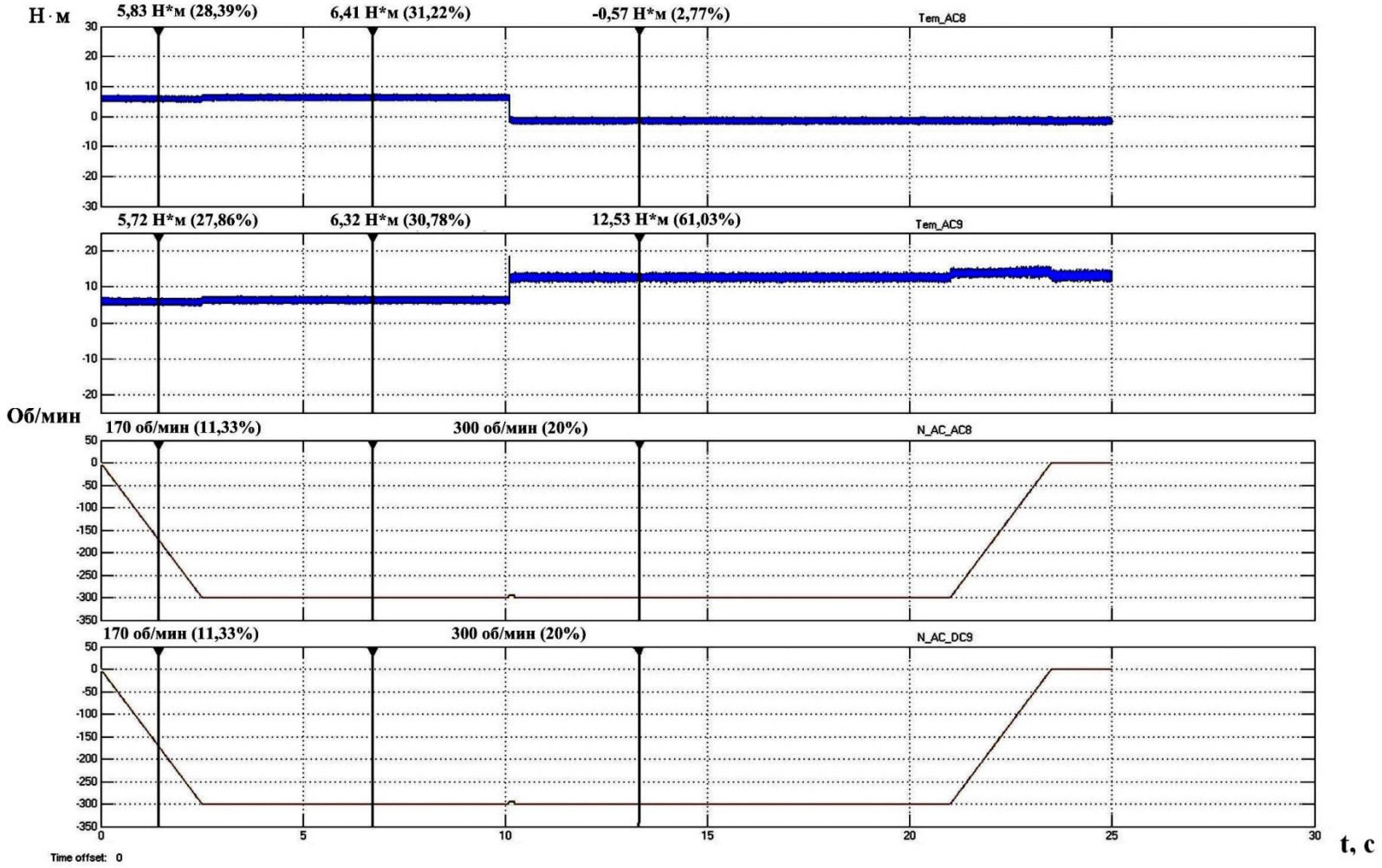

Figure 2.12 - Uniform load distribution in the mode of cargo descent with the use of SVN "lead-lead" and simulation of mechanical connection breakage (SIMULINK)

The obtained calculation result is compared, processed and used as a component of the additional task So in the control system of the "adjustable" converter. Accordingly, after determining the resulting value and its sign, the received signal of the additional task is fed to the input of the adder Σ3, where the final formation of the given moment occurs $T_{\Sigma 3}$.

Thus, the proposed technical solution fully meets the requirements of the leading-leading I / O algorithm, imposes minimal software requirements, and does not create a significant load on the operation of the converter microprocessor, which eliminates the need for additional equipment.

Inference: The obtained results confirm the principles and dependences from the classical theory of electric drives and allow us to state that the model is not only similar, but also adequate to the physical analogue, and the results can be used for comparative analysis and construction of more complex models at the next stages of research.

Further, a mathematical Simulink model was developed and assembled for a frequency-controlled twin-engine electromechanical system of an asynchronous electric drive with rigid mechanical coupling, taking into account the real discrepancy between the parameters and mechanical characteristics of the tested engines. During the tests, the causes and dependencies of the formation of the process of uneven load distribution, including the transition to the generator mode for a frequency-controlled electric drive with vector control and speed feedback, were determined. In addition, the fact of the influence of gap formation and elasticities of gears on the process of formation of an imbalance of moments was established..

Thus, in the classical open unregulated systems of an asynchronous electric drive, the uneven distribution of moments is determined by the non-identical mechanical characteristics of one type of motor. In turn, in a multi-motor, mechanically interconnected frequency-controlled drive with vector control system, the causes of unevenness are the non-identity of the specified control parameters during the transition process, the presence of an operating system, as well as an additional negative effect caused by the presence of gaps and elasticities in the mechanical part of the electric drive.

Based on the foregoing, a prerequisite for improving the operation of vector systems is to maintain a balance of the proportional distribution of the total load, due to the optimization and synchronization of the transient parameters, the presence in the control system converters of an additional circuit of the system of dynamic and static load balancing.

Modeling of the electromechanical system showed that a twin-motor asynchronous drive with a gear generates a significant imbalance in the distribution of the total load between the drives and reaches 13-20%, which indicates the need to supplement the control system with an SVN circuit; tests of the lead-to-lead IEDs on the hoist mechanism confirmed high technical indicators of load distribution, both in static and in transient operation. The accuracy of the load distribution, as in the experiments, is ~ 1-2%. Owing to the introduced structural changes and the use

of the developed “lead-lead” IOS, the vibration and vibrations of the GP mechanism are significantly reduced, and, therefore, the durability has increased.

Conclusion

As a result of dissertation research, the following results were obtained:

− the analysis of the main directions of research and development in the field of creating multi-engine interconnected electric drives;

− a mathematical model of the electromechanical system of the silo mechanism was developed taking into account the actual variation of the parameters of electric motors;

− simulation was performed and the IOS was developed in static and dynamic modes of operation of an interconnected multi-motor frequency-controlled asynchronous electric drive;

- As a result of experimental studies, it was found that the use of a leading-leading STS on the mechanism of the main hoist can reduce the moment imbalance between the drives in static and dynamic operating modes from ~ 98% to ~ 2%.

And also, on the example of an electric drive ШПТМ type НКМЗ 2Ц-5 * 2,3, the problem of energy saving and modernization of the circuit using rotary frequency converters is considered, which led to a decrease in losses of 9.8% and increased energy efficiency.

The final chapter provides options for the use of electric drives:

a) with asynchronous motor FR and transistor voltage inverters;

b) with connection of the stator FR induction motor to the 6kV 50 Hz network via a contactor reverser and a regenerative inverter in the rotor;

c) with a short-circuited stator HELL FR and a regenerative inverter in the rotor;

d) with a regenerative low-voltage inverter in the stator AM FR and a regenerative low-voltage inverter in the rotor;

f) double power machines (TIR) in the electric drive of a mine lifting machine.

Recommended literature

1) И.Я.Браславский, З.Ш.Ишматов, В.Н.Поляков. Энергосберегающий асинхронный электропривод. – Москва: Academa, 2004г.

2) Народицкий А.Г. Современное и перспективное алгоритмическое обеспечение частотно-регулируемых электроприводов. – Москва, 2014г.

3) Автоматизированный электропривод типовых производственных механизмов. М.И.Аксенов, А.И.Нитиевская, Г.Б.Онишенко. – М.:Наука, 2011г.

4) Копылов И.П. Электрические машины, часть 1. – Москва, 1986г.

5) Афонин В. И. Современные системы регулируемого лифтового привода //Тр. двенадцатой научно-технической конференции «Электроприводы переменного тока». - Екатеринбург, 2001. - С. 165-168.

6) https://erasib.ru/otraslevye-resheniya/ugol/shakhtnaya-podemnaya-mashina/eratonfr-hoist/

7) Афонин В. И., Сморженков Г. В., Фу мм Г. Я. Асинхронные двигатели регулируемых приводов лифтов //Тр. двенадцатой научно-технической конференции «Электроприводы переменного тока». - Екатеринбург, 2001.-С. 31-34.

8) Браславский И. Я. О снижении энергопотребления асинхронных электроприводов с тиристорными преобразователями напряжения// Электричество. - 1988. - № 11. - С. 58-60.

9) Браславский И. Я. О возможностях энергосбережения при использовании регулируемых асинхронных электроприводов.- Электротехника. - 1998. -№ 8. - С. 2-5.

10) Жежеленко И. В. Показатели качества электроэнергии на промышленных предприятиях. - М.: Энергия, 1977.- 128 с.

11) Жемеров Г. Г. Тиристорные преобразователи частоты с непосредственной связью. -М.: Энергия, 1977. - 280 с.

12) Ильинский Н. Ф. Основы электропривода: Учеб. пособие для вузов. - М.: МЭИ, 2000. - 164 с.

13) Шрейнер Р. Т., Поляков В. Н. К расчету оптимального по минимуму потерь закона частотного управления асинхронным электродвигателем //Асинхронный тиристорный электропривод. - Свердловск: УПИ, 1971. С. 96-98.

14) http://sibac.info

15) http://erasib.ru

16) Баклин В.С., Гимпельс А.С. Математическая модель частотно-регулируемого АД . Известия ТПУ, 2005г.